Received: April 08, 2023; **Accepted:** October 26, 2023.
DOI. 10.30473/coam.2023.67540.1230
Winter-Spring (2024) Vol. 9, No. 1, (97-130)
Research Article

Open Access

Control and Optimization in Applied Mathematics - COAM

Optimizing Supply Chain Design for Sustainability and Reliability: A Comparative Study of Augmented Epsilon and Normalized Normal Constraint Methods

Sajad Amirian, Maghsoud Amiri ✉, Mohammad Taghi Taghavifard

Department of Industrial Management, Faculty of Management and Accounting, Allameh Tabataba'i University, Tehran, Iran.

✉ **Correspondence:**
Maghsoud Amiri
E-mail:
amiri@atu.ac.ir

Abstract. Integrating sustainability and reliability represents a synergistic approach that can be explored through the problem of a closed-loop supply chain network design (SCND). This study is conducted in three stages: mathematical modeling, model solution using exact methods, and evaluation of the solution methods. In the first stage, a mixed-integer linear programming (MILP) model is developed in a multi-objective, multi-product, and multi-period framework. The objectives of the proposed model aim to maximize profitability, social responsibility, and reliability. In the second stage, two methods, namely Augmented ε-Constraint (AEC) and Normalized Normal Constraint (NNC), are implemented in the GAMS software to solve the model and identify the optimal Pareto solutions. In the third stage, the Shannon Entropy technique is employed to determine the criteria weights, and the VIKOR technique is utilized to select the superior solution method. The overall performance accuracy of the proposed model is measured using four samples from a numerical example with randomly generated data based on the objective function coefficients. The results indicate the presence of a conflict among the three objective functions. Consequently, decision-makers should consider sacrificing some profitability to enhance environmental protection and improve reliability. In terms of three criteria, run time, diversification metric, and general distance, the NNC method is given priority over the AEC method. Even when the criteria are given equal weight, the superiority of the NNC method remains unchanged. The application of the proposed model across different industries represents a significant research direction for future research.

Keywords. Supply chain network design (SCND), Sustainability, Reliability, Augmented ε-constraint (AEC), Normalized normal constraint (NNC).

MSC. 90B25; 90B50.

How to Cite
Amirian, S., Amiri, M., Taghavifard, M.T. (2024). "Optimizing supply chain design for sustainability and reliability: A comparative study of augmented epsilon and normalized normal constraint methods", Control and Optimization in Applied Mathematics, 9(1): 97-130.

1 Introduction

The decision-making process of the SCND problem to meet stakeholders' needs, and increase profitability, flexibility, and competitive advantage requires a balanced program that considers all three dimensions of sustainability [2]. One of the most essential quality goals for businesses is to avoid production interruptions and service disruptions such as incomplete and delayed delivery of goods/services. Due to the diversity in nature and equipment, the supply chain may experience various failures. The failure of one component of the supply chain network may disrupt the performance of the entire supply chain or, at best, reduce the chain's efficiency. The complete and healthy delivery of products to customers in the supply chain requires the failure-free operation of facilities, communication routes, and vehicles as components of the supply chain network. However, reliability in SCND is evaluated at the level of network facilities. Facility reliability and resilience against disruption conditions are among the recent developments that researchers have added to sustainable supply chains [26]. Therefore, it seems necessary to consider the reliability factor in the supply chain design, especially in sustainable supply chains.

In many supply chains, sustainable and reliable designs are done to achieve a cleaner environment, fair distribution of resources and benefits in society, and strengthen supply security by providing affordable products and services to customers. However, resource limitations do not allow these goals to be achieved simultaneously, as achieving each of them requires a trade-off with the other [5]. Therefore, a challenge arises in integrating sustainability and reliability in SCND. The traditional approach to this challenge has been to accept trade-offs between these goals. However, integrating sustainability and reliability as a new paradigm can implement sustainability policies and reliability strategies. Torjai et al. [48] discuss the cooperation between these two paradigms and claim that reliability as an enabler can enhance sustainability by influencing cost-effectiveness. Similarly, Ghobakhloo et al. [20] found that only when both paradigms were implemented simultaneously could sustainability and reliability reveal their full potential and generate more benefits than when they are implemented separately, creating a synergy. Therefore, with the motivation of addressing the concerns above, and given that the combination of sustainability and reliability has become a popular paradigm in recent years, the present study aims to consider both of these critical features in the closed-loop SCND. To achieve this goal, a multi-objective, multi-product, and multi-period mathematical model is developed. The proposed model seeks to maximize total profit, social responsibility, and reliability while complying with environmental considerations using the cap and trade mechanism. Materials and products are transported using heterogeneous fleets with differences in capacity, fuel consumption, and CO_2 emissions. To evaluate social sustainability the study considers essential social responsibility criteria such as job opportunities created and working days lost from occupational injuries, as well as the area's unemployment rate to create more employment in deprived areas. In addition, the reliability category is considered by choosing suppliers, building potential facilities, reopening connection routes, and using vehicles. According to the reviewed literature, this is the first time vehicle reliability has been modeled in SCND. Therefore, this type of modeling is innovative compared to the former models and can help accurately evaluate the responsiveness of the network and the level of satisfaction of supply chain customers. The proposed model is solved using sensitivity analysis to gain some helpful management insights. By adjusting the assumptions and parameters of the proposed model, its results can be used in industries that need to consider sustainability and reliability approaches.

The study seeks to address the shortcomings of past studies as much as possible and provide a model compatible with the natural conditions of the closed-loop SCND problem, while considering sustainability and reliability. The innovations of the presented model are summarized as follows:

- Development of a mathematical model for a closed-loop SCND problem by simultaneously considering outsourcing decisions (supplier selection and order allocation), strategic decisions (determining the location, number, and capacity level of potential facilities, determining the production technology, determining the materials used in the recycling process, determining the trucks of transport) and tactical decisions (the amount of production of products, the flow of materials and products within the network, the number of products saves, the amount of shortage of inventory, the number of products returned from customers, the number of uncollected products returned, the amount of CO2 emitted)

- Paying particular attention to the social dimension of sustainability by considering the most common social criteria in past studies, such as job opportunities created and the rates of occupational injuries in the workplace in fixed (establishment of facilities) and variable (operational activities).
- Focusing on creating equity-oriented employment, considering the possibility of establishing facilities in areas with higher unemployment rates.
- A more comprehensive assessment of supply chain reliability by considering the reliability of nodes (including suppliers, manufacturers, distributors, collection centers, recycling centers, and operational activities) and the reliability of arcs (including routes and trucks of transport).
- And solving the problem with two exact solution methods, including Augmented ε-Constraint (AEC) and Normalized Normal Constraint (NNC), and comparing their performance using the VIKOR technique.

The next sections of this paper are structured as follows. Section 2 describes the background, Section 3 deals with materials and methods, Section 4 presents the results, Section 5 discusses sensitivity analysis of mathematical models and problem-solving techniques, and Section 6 is devoted to the conclusion and future research.

2 Literature Review

Prior to the emergence of reliable supply chains, the optimization of SCND was raised as an economic problem solely. Dullaert and Zamparini [11] justified the more expensive logistic structure with higher reliability through a mathematical planning model. Ghayebloo et al. [19] concluded that returned products from more reliable parts result in reduced recycling costs. Therefore, the cheapness and reliability of each facility within the supply chain have been given greater attention [43]. Hamidieh et al. [24] presented a sustainable closed-loop SCND model that minimizes total costs while maintaining network resilience and controlling delivery speed at appropriate safety levels. Fakhrzad and Goodarzian [13] sought to minimize the total cost and maximize the reliability of delivery demand in a green closed-loop SCND problem. Tirkolaee et al. [47] used weighted goal programming (WGP) to solve the three-level SCND problem, including suppliers, warehouses, and wholesalers, with the tri-objectives of minimizing the total cost, maximizing the weighted value of products by considering the suppliers' priorities, and maximizing the reliability. Nosrati and Khamseh [39] developed a two-stage stochastic programming model for the SCND problem with the objectives of maximizing reliability and minimizing cost.

Green SCND is one of the models whose purpose is to integrate economic and environmental factors in designing supply chain networks. Fazli-Khalaf et al. [15] used a scenario-based stochastic planning approach to control the adverse effects of disruptions in the proposed model in designing a reliable green closed-loop supply chain with the two objectives of reducing costs and releasing harmful gases. Rahmani and Mahoodian [42] considered the issue of designing the supply chain network regarding CO2 emissions and the reliability factor. Li et al. [31] considered the environmental aspect of sustainability through minimizing the emission or cost of environmental pollution. In addition, carbon emission mechanisms in the mathematical model of SCND include carbon cap [38], carbon tax [33], carbon cap and trade [29], and carbon offset [9]. Kabadurmus and Erdogan [28] showed that multimodal transportation reduces supply chain costs and carbon emissions. Yılmaz et al. [51] demonstrated that the effect of waves (i.e., the external side of the chain) increases supply chain costs and carbon emission by 40%. Foong and Ng [18] used the alliance reliability index to measure reliability in a palm oil SCND with economic and environmental objectives. Salehi and Jabarpour [44] used a fuzzy programming approach to solve a multi-period location-routing problem to minimize cost, lost demand, and vehicles with fuzzy routes in a forward humanitarian supply chain. The social responsibility was highlighted in Fattahi and Govindan [14] and Govindan and Gholizadeh [22].

After 2015, sustainable and reliable supply chains emerged as a new cluster in the SCND literature and other subject areas, such as environmental resilience measures [52], resilience strategies [27], minimizing resilience-reducing measures [25], which are closely linked to reliability, were identified. Empirical evidence suggests that production speed leads to more defects and frequent breakdowns of production machinery [33]. Fazli-Khalaf et al. [16], Wang et al. [50], Abir et al. [1], and Fazli-Khalaf et al. [17] integrated sustainability and reliability in the SCND problem. Basu and Lee [7] state that reliability practices act as a catalyst for sustainable outcomes, indicating enormous potential for integration. Akbari Kasgari et al. [4] used backup suppliers as a resilience strategy to reduce the effects of earthquakes on mining operations. Eslamipoor and Nobari [12] state that the capacity of the supply chain to respond to the blood needs of hospitals is a reliable means to achieve the social goal and limit the cost.

Previous studies have often examined the potential for disruption in supply chain design and logistics networks by considering facilities and transport links separately. For instance, Amirian et al. [6] presented a model for designing a closed-loop SCND that encompasses multiple objectives, products, and time periods. However, their proposed model was time-consuming to solve due to its nonlinearity. Additionally, reliability was only addressed in terms of supplier selection, potential facility implementation, and travel time in their supply chain design. In contrast to these previous works, this research simultaneously considers the reliability of facilities, the failure of network arcs, and the failure of transportation trucks within the SCND problem. Thus, the model developed in this study offers a unique and innovative approach. The primary contribution of this paper lies in the application and comparison of two solution techniques, AEC and NNC, for modeling a sustainable and reliable SCND problem.

Table 1 highlights the gaps in the literature and provides a more detailed classification of the subject by discussing additional features addressed in past studies.

3 Problem Description

In this section, we will discuss the materials and methods required to describe the problem at hand.

3.1 Research implementation process

Solving an optimization problem requires two basic steps: mathematical modeling and solving the model. These steps complement each other, and optimization has not occurred without performing each step. In addition, using different methods to solve a problem (especially multi-objective problems) often leads to different solutions. Therefore, achieving convergence in Pareto solutions and providing diverse solutions are separate and somewhat conflicting goals for multi-objective methods. Choosing the appropriate solution method for the current research problem involves determining the appropriate multi-objective approaches, solving the problem model with the determined approaches, identifying the appropriate criteria for evaluating the approaches, evaluating and comparing the approaches, and choosing the best approach for solving the sustainable and reliable SCND problem. Figure 1 illustrates the research implementation process.

Table 1: Summary of research background.

Author (year)	Network structure	Configuration				Problem conditions		Dimensions of sustainability	Levels of reliability
		Objective	Product	Period	Transportation	Modeling	Certainty		
Ghayebloo et al. (2015)	CL	M	M	S	S	L	D	DBL	N
Fazli-Khalaf et al. (2017)	CL	M	S	S	S	L	ND	DBL	N
Rahmani and Mahoodian (2017)	OL	S	M	S	M	L	ND	DBL	N
Fakhrzad and Goodarzian (2019)	CL	M	M	M	M	L	ND	DBL	N
Li et al. (2019)	OL	M	S	S	S	L	D	DBL	N
Marchi et al. (2019)	OL	S	S	S	S	L	D	DBL	N
Kaur and Singh (2019)	OL	S	M	M	M	NL	D	DBL	N
Abir et al. (2020)	CL	M	S	S	S	L	ND	DBL	N
Mousavi-Ahranjani et al. (2020)	OL	S	M	M	M	L	ND	DBL	N
Kabadurmus and Erdogan (2020)	OL	S	M	S	M	L	D	DBL	N
Nosrati and Arshadi-Khamseh (2020)	OL	M	M	S	M	NL	ND	DBL	C
Wang et al. (2020)	OL	S	S	M	M	L	D	DBL	N
Abdolazimi et al. (2020)	CL	M	M	M	S	L	ND	DBL	N
Yılmaz et al. (2021)	OL	S	M	S	S	L	ND	DBL	A
Foong and Ng (2022)	OL	M	S	S	S	L	ND	DBL	N
Fahimnia and Jabbarzadeh (2016)	OL	M	M	S	M	L	ND	TBL	N
Zahiri et al. (2017)	OL	M	M	M	M	L	ND	TBL	N
Fattahi and Govindan (2018)	OL	S	S	M	M	L	ND	TBL	N
Jabbarzadeh et al. (2018)	OL	M	S	S	S	L	ND	TBL	N
Zare Mehrjerdi and Lotfi (2019)	CL	M	M	M	S	L	ND	TBL	N
Fazli-Khalaf et al. (2020)	OL	M	M	M	M	L	ND	TBL	N
Hosseini-Motlagh et al. (2020)	OL	M	S	M	S	L	ND	TBL	C
Babaee Tirkolaee et al. (2020)	OL	M	M	M	S	L	ND	TBL	N
Tsao and Thanh (2020)	OL	M	S	M	S	L	ND	TBL	A
Fazli-Khalaf et al. (2021)	CL	M	S	S	S	L	ND	TBL	N
Lotfi et al. (2021)	CL	M	M	M	S	L	ND	TBL	N
Zare Mehrjerdi and Shafiee (2021)	CL	M	M	S	S	L	ND	TBL	N
Sadeghi et al. (2021)	OL	M	M	S	S	L	ND	TBL	N
Govindan and Gholizadeh (2021)	OL	S	M	M	S	L	ND	TBL	N
Sazvar et al. (2021)	OL	M	S	M	M	L	ND	TBL	N
Akbari-Kasgari et al. (2022)	CL	M	M	S	S	L	D	TBL	N
Amirian et al. (2022b)	CL	M	M	M	M	NL	D	TBL	C
Salehi et al. (2022)	OL	S	M	M	S	L	ND	TBL	N
Taleizadeh et al. (2022)	CL	M	S	S	S	L	D	TBL	N
Goodarzian et al. (2022)	OL	M	M	M	M	L	ND	TBL	N
Mohammadi and Nikzad (2022)	CL	M	M	M	S	L	ND	TBL	N
This study	CL	M	M	M	M	L	D	TBL	C

Table guide
Network structure (OL: Open-Loop, CL: Closed-Loop); Configuration (S: Single, M: Multiple); Problem Conditions: Modeling (L: Integer Linear Mixed Programming, NL: Integer nonlinear Mixed Programming); Model certainty (D: Deterministic, ND: Non-Deterministic); Sustainability level: (1D: SBL, 2D: DBL, 3D: TBL); Reliability Level: (N: Node, A: Arc, C: Chain)

3.2 Problem definition

The current research mathematically models a reliable, cheap, closed-loop SCND problem while prioritizing social responsibility and consumer satisfaction. Supply chains can make strategic decisions regarding the location of potential facilities such as production, distribution, collection, and recycling centers, as well as tactical decisions related to the flow rate of materials and goods in the chain, with

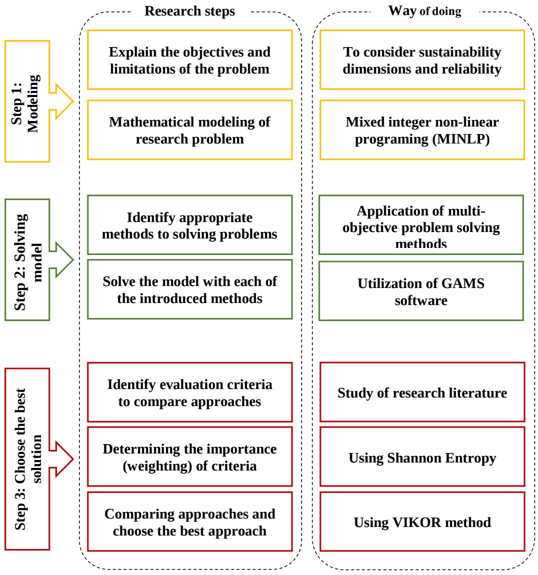

Figure 1: Field and steps of study implementation.

the aim of achieving profitability, social responsibility, and excellent reliability. To this end, a MILP model has been developed. The presented model is suitable for most industries that have a social responsibility for collecting end-of-life products from customers, such as pharmaceuticals, dairy products, non-rechargeable batteries, car tires, etc. The proposed supply chain network includes suppliers, manufacturers, distributors, and direct customers, collection centers, recycling centers, energy recovery centers, markets for recycled raw materials, and disposal centers in the reverse chain. Customers or final consumers issue the primary demand in this structure. It assumed that there is no special relationship between the components of a particular chain level. In other words, each component is independent of others, and there is no exchange of goods between subsystems. The location of suppliers and customers is fixed. Additionally, production, distribution, collection, and recycling centers can be set up in three different capacities (such as small, medium, and large sizes), with varying fixed setup costs associated with each capacity level. Figure 2 illustrates the investigated supply chain structure.

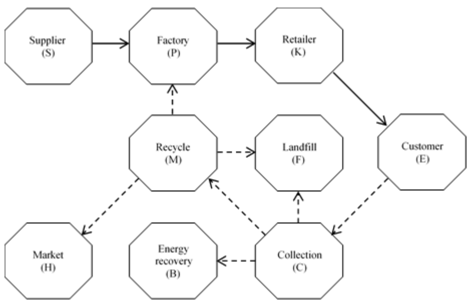

Figure 2: Proposed closed-loop supply chain structure.

In the direct chain, raw materials are procured from suppliers and factories use a specific combination of these materials to produce goods that are shipped to distribution centers. The distribution centers are responsible for storing and delivering the products to end customers. In the reverse supply chain, used products are returned from the demand centers to collection centers, where they are examined and separated into three categories based on their quality: high value, low value, and worthless (determined by the time used). Valuable parts are sent to recycling centers for reuse, low-value parts are sold to energy recovery centers, and worthless parts are sent to disposal centers for safe burial. According to the materials used in the recycling, the recycled raw materials are divided into two parts: raw materials suitable for production and raw materials suitable for sale in the secondary market. To move raw materials and products between different levels of the supply chain, heterogeneous vehicles are used. To account for the natural conditions of the problem, failure modes are defined for facilities, routes, and trucks of transportation. The impact of these failures on the reliability of the supply chain is discussed in the model. A reliability index is considered for each supply chain facility, which shows the probability of correct operation without failure in a certain period. This index depends on investment amount, design power, and degree of flexibility. Facilities with higher flexibility have higher reliability. In addition, the reliability of distribution and collection centers depends significantly on their storage systems and separation capabilities. The faster they respond, the more reliable they are. Production technology, product storage technology, and materials used in recycling vary from one facility to another. The reliability of transportation activities is measured by considering the probability of failure for the communication routes and the vehicles used based on the distance traveled between the facilities.

Table 2: Definition of sets, parameters, and variables.

Category	Symbol	Description
		Sets
Main	S	Set of suppliers $s \in S$
	P	Set of potential production centers $p \in P$
	K	Set of potential distribution centers $k \in K$
	E	Set of primary market $e \in E$
	C	Set of potential collection centers $c \in C$
	M	Set of potential recycling centers $m \in M$
	H	Set of the secondary market for recycled raw material $h \in H$
	F	Set of landfill centers $f \in F$
	B	Set of energy recovery centers $b \in B$
	A	Set of raw materials $a \in A$
	R	Set of products $r \in R$
	L	Set of materials used in recycling process $l \in L$
	G	Set of technologies in production centers $g \in G$
	V	Set of vehicle$v \in V$
	U	Set of usable capacity $u \in U$
	D, T	Set of period $t, d \in T$
Hybrid	N	Set of network nodes $N \in \{s, p, k, e, c, m, b, f, h\}$
	Φ	Set of network arcs $\Phi(x,y) \in \left\{ \begin{array}{l} 1:(s,p), \Phi_2:(p,m), \Phi_3:(m,h), \Phi_4:(p,k),) \\ (\Phi_5:(k,e), \Phi_6:(e,c), \Phi_7:(c,m), \Phi_8:(c,b), \Phi_9:(c,f) \end{array} \right\}$
	$\Phi^{'}$	Set of arcs for carrying raw materials $\Phi^{'} \subset \Phi; \Phi^{'} \in \{\Phi_1, \Phi_2, \Phi_3\}$
	$\Phi^{''}$	Set of arcs for carrying products $\Phi^{''} \subset \Phi; \Phi^{''} \in \{\Phi_4, \Phi_5, \Phi_6, \Phi_7, \Phi_8, \Phi_9\}$
		Parameters
prices	PR_{er}^{t}	The selling price of one unit of product r in primary market e in period t
	PR_{br}^{t}	The selling price of one unit of returned product r in energy recovery center b in period t
	PR_{ha}^{t}	The selling price of one unit of recycled raw material a in the secondary market h in period t
Fixed costs	F_{p}^{gu}	Fixed cost of establishing one production center p with technology g and capacity level u
	F_{k}^{u}	Fixed cost of establishing one distribution center k with a capacity level u
	F_{c}^{u}	Fixed cost of establishing one collection center c with a capacity level u
	F_{m}^{lu}	Fixed cost of establishing one recycling center m using materials l and capacity level u
	F_{sa}^{t}	Fixed cost of obtaining a contract with supplier s for the supply of raw material a in period t
	F_{v}^{t}	Fixed cost of using vehicle v in period t
	Θ	Fixed cost of limiting emission of carbon dioxide

Unit costs	BC_{sa}^{t}	Purchasing cost for one unit of new raw material a from supplier s in period t
	RC_{a}^{t}	Cost savings from recycling one unit of raw material a in a period of t
	PC_{pr}^{gt}	Producing cost one unit of product r in the production center p with technology g in period t
	KC_{kr}^{t}	Distributing cost of one unit product r at the distribution center k in period t
	HC_{kr}^{t}	Maintaining cost of one unit product r in the distribution center k in period t
	EC_{er}^{t}	Penalty for lack of one unit product r in period t
	OEC_{er}^{t}	Penalty for non-collection of one unit returned product r from customer e in period t
	CC_{cr}^{t}	Cost of separating and packing per returned product r in collection center c in period t
	OCC_{cr}^{t}	Incentive cost to purchase and collect per returned product r at collection center c in period t
	MC_{mr}^{lt}	Recycling cost per returned product r in recycling center m using material l in period t
	FC_{fr}^{t}	Destroying cost of one unit of returned product r in destruction center f in period t
	V_{v}^{t}	Cost per liter of fuel consumed for vehicle v in period t
	F_{d}^{t}	Driver's wages per hour of driving in period t
Capacities	Cap_{sa}	Capacity of supplier s of raw materials a
	Cap_{p}^{gu}	The capacity of production center p with technology g and capacity level u
	Cap_{k}^{u}	The capacity of distribution center k with capacity level u
	VCap_{k}^{u}	Storage capacity of distribution center k with capacity level u
	Cap_{c}^{u}	The capacity of collection center c with capacity level u
	Cap_{m}^{lu}	The capacity of recycling center m using material l and capacity level u
	WCap^{v}	Weight capacity of vehicle type v
	VCap^{v}	Volume capacity of vehicle type v
Carbon dioxide	$\mathrm{CO}_{2}^{\mathrm{GOV}}$	The amount allowable of CO2 emissions by the government for the supply chain network
	E_{p}^{gu}	Fixed CO2 emissions from establishing production center p with technology g and capacity level u
	E_{k}^{u}	Fixed CO2 emissions from establishing distribution center k with a capacity level of u
	E_{c}^{u}	Fixed CO2 emissions from establishing collection center c with a capacity level of u
	E_{m}^{lu}	Fixed CO2 emissions from establishing a recycling center m using material l and capacity level u
	ϵ^{J}	Emission rate of CO2 per one unit of energy consumed (g/kwh)
	ϵ^{l}	Emission rate of CO2 per one liter of fuel consumed (g/Liter)
Energy and fuel	EP_{r}^{g}	Energy consumed to produce one unit of product r with technology g (kWh)
	EK_{r}	Energy consumed to distribute one unit of product r (kWh)
	EC_{r}	Energy consumed to collect one unit of returned product r (kWh)
	EM_{a}^{l}	Energy consumed to recycle one unit of raw material a with material l (kWh)
	EB_{r}	Energy consumed to recover energy from one unit of returned product r (kWh)
	EF_{r}	Energy consumed for burying one unit of returned product r (kWh)
	$\mathrm{FU1}_{v}$	Fuel consumed per kilometer traveled by the vehicle v in no-load mode (Liter)
	$\mathrm{FU2}_{v}$	Fuel consumed per kilometer traveled by the vehicle v with one unit load (Liter)
Employment	θ_{job}	The importance coefficient of job opportunities created
	job_{p}^{gu}	Job opportunities from establishing production center p with technology g and capacity level u
	job_{k}^{u}	Job opportunities from establishing of distribution center k with capacity level u
	job_{c}^{u}	Job opportunities from establishing of collection center c with capacity level u
	job_{m}^{lu}	Job opportunities from establishing a recycling center m using material l and capacity level u
	η_{p}	The unemployment rate in the production center p
	η_{k}	Unemployment rate in the distribution center k
	η_{c}	Unemployment rate in the collection center c
	η_{m}	Unemployment rate in recycling center m
	jt	Variable rate of job creation per hour of operational activity
Occupational injuries	θ_{ltc}	Importance coefficient of sick leave
	ltc_{p}^{gu}	Occupational injuries from the establishment of production center p, technology g, and capacity level u (days)
	tc_{k}^{u}	Occupational injuries from the establishment of distribution center k with capacity level u (days)
	ltc_{c}^{u}	Occupational injuries from the establishment of collection center c with capacity level u (days)
	ltc_{m}^{lu}	Occupational injuries from the establishment of recycling center m, material l, and capacity level u (days)

	lt	Variable rate of occupational injuries per hour of operational activity
Reliability	λ_1	Importance coefficient of supplier reliability
	λ_2	Importance coefficient of potential facility establishment reliability
	λ_3	Importance coefficient of operational activities reliability
	λ_4	Importance coefficient of shipment reliability
	SR_{sa}	Reliability of supplier s in supplying raw materials a
	RP_n^{gu}	Reliability of production center p with technology g and capacity level u
	RK_n^{u}	Reliability of distribution center k with capacity level u
	RC_n^{u}	Reliability of collection center c with capacity level u
	RM_n^{lu}	Reliability of recycling center m using material l and capacity level u
Failure rate	λ_v	Breakdown rate of vehicle v per kilometer traveled
	λ_{xy}	Breakdown rate of arc between x and y per kilometer
	λ_p^{gut}	Breakdown rate of production center p with technology g and capacity level u in period t
	λ_k^{ut}	Breakdown rate of distribution center k with capacity level u in period t
	λ_c^{ut}	Breakdown rate of collection center c with capacity level u in period t
	λ_m^{lut}	Breakdown rate of recycling center m using material l and capacity level u in period t
Coefficients of distance, time, weight, and volume	D_{xy}	The distance between each pair of nodes x and y in the supply chain (Kilometer)
	D_r	Maximum helpful life of product r
	TP_r^g	Required time to produce one unit of product r using technology g
	TK_r	Required time for distributing one unit of product r
	TC_r	Required time for collecting one unit of product r
	TM_a^l	Required time for recycling one unit of raw material a using material l
	w_a	The weight per unit of raw material a
	w_r	The weight per unit of product r
	v_a	The volume per unit of raw material a
	v_r	The volume per unit of product r
other coefficients	b_{sa}^t	Minimum supply of raw material a by supplier s in period t
	Dem_{er}^t	The demand of primary market e for product r in period t
	q_{ar}	Ratio using of raw material a in product r; $\sum_{a\in A} q_{ar}=1, \forall r\in R$
	ρ_{ar}	Extraction ratio of raw material a per returned product r; $\sum_{a\in A}\rho_{ar}=1,\forall r\in R$
	β_r	The energy recovery ratio per returned product r
	γ_r	Recycle ratio of per returned product r; $\beta_r+\gamma_r<1,\forall r$
	σ_a	The reused ratio of recycled raw material a
	ω_r^d	Returned rate of the end-of-life product r after d years of use; $\sum_{d=0}^{D_r}\omega_r^d\le 1$
	Budget	The budget total available for the establishment of potential facilities
	BM	The big number
		Decision variables
Binary variable	θ_{sa}^t	One, If concluded a contract of supply of raw material a with supplier s in period t; Otherwise, zero
	θ_p^{gu}	One, If established a production center p with technology g and capacity level u; Otherwise, zero
	θ_k^u	One, If established a distribution center k with capacity level u; Otherwise, zero
	θ_c^u	One, If established a collection center c with capacity level u; Otherwise, zero
	θ_m^{lu}	One, If established a recycling center m using material l and capacity level u; Otherwise, zero
	π_{xy}^{vt}	One, If vehicle v travels arc x to y in period t; Otherwise, zero
Positive variable	Q_{xya}^t	Quantity transferred of raw material a between the facilities $(x,y)\in\Phi'$ in period t
	Q_{xyr}^t	Quantity transferred of product r between the facilities $(x,y)\in\Phi''$ in period t
	Q_{pr}^{gt}	Quantity produced of product r in production center p with technology g in period t
	I_{kr}^t	Quantity held inventory of product r in distribution center k in period t
	QR_{xr}^t	Quantity returned product r from customer e in period t
	QN_{er}^t	Quantity uncollected of returned product r from customer e in period t
	S_{er}^t	Quantity lack of product r for customer e in period t
	CO_2^{CUR}	Quantity of carbon dioxide emissions in the supply chain (tons)

3.3 Problem modeling

This section presents a mathematical representation of the problem. A prerequisite for mathematical modeling is the identification of symbols, parameters, and variables that accurately describe the problem's characteristics.

3.3.1 Symbolization

This section introduces the symbols, parameters, and variables used in the mathematical model. Table 2 provides a simplified view of the mathematical model by grouping similar symbols, parameters, and variables together for easier reference.

3.3.2 Assumptions

The assumptions of the problem include:

- The closed-loop SCND model is multi-product, multi-objective, and multi-period.
- There is no flow between facilities at one level of the chain.
- Final products are traded in the primary (forward chain) market, and recycled raw materials are traded in the secondary (reverse chain) market.
- The useful life of final products is limited regarding time.
- Lost demand for finished products is subject to penalties.
- No collecting returned products will be fined.
- Potential facilities are established with only one level of capacity.
- Heterogeneous vehicles are used to transport raw materials and final products.

3.3.3 Mathematical model

This study modeled sustainable and reliable SCND as a multi-objective problem. Supply chain sustainability is pursued in the model by considering the two objectives of green investment and social responsibility. Reliability of product delivery, which aims to achieve customer satisfaction, is the third goal pursued as the third objective function. Therefore, all three objective functions in the mathematical model are of the maximization type, described below.

Profitability Objective

The first objective function seeks to maximize profitability. Equation (1) shows the first objective function. Equation (2) calculates the total income. Total income is calculated by adding up the final products sold to the primary market, returned products sold to energy recovery centers, and recycled raw materials sold to the secondary market. Equation (3) calculates the total costs. The total costs are calculated by summing up fixed, operating, transportation, and CO2 emissions costs.

$$\text{Maximize} \qquad Z1 = \text{Economic Profit (EP)} = \text{Total Revenue (TR)} - \text{Total Cost (TC)} \tag{1}$$

$$\begin{aligned} \text{TR} = \sum_{t\in T}\Bigg[& \sum_{(x,y)\in\Phi_5}\sum_{r\in R}\text{PR}^t_{er}\cdot Q^t_{xyr} + \sum_{(x,y)\in\Phi_8}\sum_{r\in R}\text{PR}^t_{br}\cdot Q^t_{xyr} \\ & + \sum_{(x,y)\in\Phi_3}\sum_{a\in A}\text{PR}^t_{ha}\cdot Q^t_{xya}\Bigg], \end{aligned} \tag{2}$$

$$\begin{aligned} \text{TC} = {} & \text{Fixed Cost (FC)} + \text{Operation Cost (OC)} + \text{Shipping Cost (SC)} \\ & + \text{Emission Cost (EC)}. \end{aligned} \tag{3}$$

Equation (4) calculates fixed costs from the sum of the establishment cost of potential facilities, the supplier's contracting cost, and the route's reopening cost. Facility capacity, production technology, and materials used to recycle raw materials impact potential facility establishment fixed costs [25]. Changing the cost of raw material supply contracts in different periods is possible based on market conditions. The fixed cost of using cargo trucks may change in different periods.

$$\begin{aligned} C = \sum_{u\in U}\Bigg[& \sum_{n\in P}\sum_{g\in G}F^{gu}_n\cdot\theta^{gu}_n + \sum_{n\in K}F^u_n\cdot\theta^u_n + \sum_{n\in C}F^u_n\cdot\theta^u_n + \sum_{n\in M}\sum_{l\in L}F^{lu}_n\cdot\theta^{lu}_n\Bigg] \\ & + \sum_{n\in S}\sum_{a\in A}\sum_{t\in T}F^t_{na}\cdot\theta^t_{na} + \sum_{(x,y)\in\Phi}\sum_{v\in V}\sum_{t\in T}F^t_v\cdot\pi^{vt}_{xy}. \end{aligned} \tag{4}$$

Equation (5) shows the supply chain operational costs, which include variable costs related to performing activities in each of the facilities.

$$\begin{aligned} \text{OC} = \sum_{t\in T}\Bigg[& \sum_{(x,y)\in\Phi_1}\sum_{a\in A}\text{BC}^t_{sa}\cdot Q^t_{xya} - \sum_{(x,y)\in\Phi_2}\sum_{a\in A}\text{RC}^t_a\cdot Q^t_{xya} \\ & + \sum_{p\in P}\sum_{r\in R}\sum_{g\in G}\text{PC}^{gt}_{pr}\cdot Q^{gt}_{pr} + \sum_{(x,y)\in\Phi_5}\sum_{r\in R}\sum_{v\in V}\text{KC}^t_{kr}\cdot Q^t_{xyr} + \sum_{k\in K}\sum_{r\in R}\text{HC}^t_{kr}\cdot I^t_{kr} \\ & + \sum_{e\in E}\sum_{r\in R}(EC^t_{er}\cdot S^t_{er} + OEC^t_{er}\cdot QN^t_{er}) + \sum_{(x,y)\in\Phi_6}\sum_{r\in R}(CC^t_{cr} + OCC^t_{cr})\cdot Q^t_{xyr} \\ & + \sum_{(x,y)\in\Phi_7}\sum_{r\in R}\sum_{l\in L}MC^{lt}_{mr}\cdot Q^t_{xyr} + \sum_{(x,y)\in\Phi_9}\sum_{r\in R}FC^t_{fr}\cdot Q^t_{xyr}\Bigg]. \end{aligned} \tag{5}$$

Equation (6) calculates shipment costs by adding up the fuel cost and vehicle use. Fuel consumption depends on the vehicle type, the load carried, and the distance traveled [8]. The cost of transportation is calculated based on travel time. Travel time is a function of the vehicle speed and the distance traveled.

$$\begin{aligned} \text{SC} = \sum_{v\in V}\sum_{t\in T}\Bigg[& \sum_{(x,y)\in\Phi'}\sum_{a\in A}D_{xy}\pi^{vt}_{xy}\cdot((V^t_v(FU1_v + (FU2_v\cdot W_a\cdot Q^t_{xya})) + ((F^t_d)/(V^v)))\Bigg] \\ & + \Bigg[\sum_{(x,y)\in\Phi''}\sum_{r\in R}D_{xy}\pi^{vt}_{xy}\cdot((V^t_v(FU1_v + (FU2_v\cdot W_r\cdot Q^t_{xyr})) + ((F^t_d)/(V^v)))\Bigg]. \end{aligned} \tag{6}$$

The measure of transportation CO2 emissions is complicated by various factors such as the shipment mode, type of fuel used, load weight, and distance traveled [45]. Despite this complexity, calculations of GHG emissions in literature are not always straightforward due to their simplicity in calculation. For example, Mirzapour Al-e-hashem and Rekik [37] considered only the distance traveled, while Bektaş and Laporte [8] and Liu et al. [32] took into account vehicle speed and freight volume.

Equation (7) calculates the CO2 emissions cost of the supply chain, which may exceed the government's limit if it exceeds the allowed emission cap determined by mechanisms such as carbon taxes or caps, carbon cap and trade, and carbon offset. This penalty cost is represented by the symbol Θ in

Equation (7). Equation (8) shows how the fixed and variable costs associated with CO2 emissions are calculated, respectively. Equation (9) is related to the fixed part (i.e., CO2 emissions from the facility establishment), while Equation (10) is related to the variable part (i.e., CO2 emissions from the energy consumed). Equation (11) calculates the energy consumed in operational processes, and Equation (12) calculates the energy consumed in network shipment.

$$\mathrm{EC} = \Theta(\mathrm{CO}_2^{CUR} - \mathrm{CO}_2^{\mathrm{GOV}}), \tag{7}$$

$$\mathrm{CO}_2^{\mathrm{CUR}} = \text{Fixed Emission CO}_2(\text{FEC}) + \text{Variable Emission CO}_2(\text{VEC}), \tag{8}$$

$$\mathrm{FEC} = \sum_{u\in U}\Big[\sum_{p\in P}\sum_{g\in G} E_p^{gu}\cdot\theta_p^{gu} + \sum_{k\in K} E_k^u\cdot\theta_k^u + \sum_{c\in C} E_c^u\cdot\theta_c^u + \sum_{m\in M}\sum_{l\in L} E_m^{lu}\cdot\theta_m^{lu}\Big], \tag{9}$$

$$\begin{aligned}\mathrm{VEC} = {} & \epsilon^j\cdot[\text{Consumption Energy Operation (CEO)}]\\ & + \epsilon^l\cdot[\text{Consumption Energy Shipping (CES)}],\end{aligned} \tag{10}$$

$$\begin{aligned}\mathrm{CEO} = {} & \sum_{r\in R}\sum_{t\in T}\Big[\sum_{p\in P}\sum_{g\in G} EP_r^g\cdot Q_{pr}^{gt} + \sum_{(x,y)\in\Phi_5} EK_r\cdot Q_{xyr}^t\\ & + \sum_{(x,y)\in\Phi_6} EC_r\cdot Q_{xyr}^t + \sum_{(x,y)\in\Phi_7}\sum_{a\in A}\sum_{l\in L} EM_a^l\cdot\rho_{ar}\cdot Q_{xyr}^t\\ & + \sum_{(x,y)\in\Phi_8} EB_r\cdot Q_{xyr}^t + \sum_{(x,y)\in\Phi_9} EF_r\cdot Q_{xyr}^t\Big],\end{aligned} \tag{11}$$

$$\begin{aligned}\mathrm{ES} = {} & \sum_{v\in V}\sum_{t\in T}\Big[\sum_{(x,y)\in\Phi'}\sum_{a\in A} D_{xy}\cdot\pi_{xy}^{vt}(FU1_v + (FU2_v W_a Q_{xya}^t)\Big]\\ & + \Big[\sum_{(x,y)\in\Phi''}\sum_{r\in R} D_{xy}\cdot\pi_{xy}^{vt}(FU1_v + (FU2_v W_r Q_{xyr}^t)\Big].\end{aligned} \tag{12}$$

Social Responsibility Objective

In terms of sustainability based on the ISO 26000 standard, various criteria cannot be fully addressed by one single study. However, in this research, the most commonly used criteria are those presented in previous studies such as Equation (13) which maximizes the social responsibility within the supply chain. Social responsibility is calculated by subtracting the number of jobs created from the number of sick leave days taken for each period. The ultimate goal is to establish facilities in areas with higher unemployment rates and provide more job opportunities in deprived regions, as per Equation (14). Equation (15) calculates employees' sick leaves. These criteria are adapted from the study conducted by Fazli-Khalaf et al. [16].

$$\text{Corporate Social Responsibility (CSR)} = \theta_{\text{job}}\times[\text{Jobs Created (JC)}] - \theta_{\text{ltc}}\times[\text{Lost Days (LD)}] \tag{13}$$

$$\begin{aligned}\mathrm{JC} = {} & \sum_{u\in U}\Big(\sum_{p\in P}\sum_{g\in G}\eta_p\cdot\mathrm{job}_p^{gu}\cdot\theta_p^{gu} + \sum_{k\in K}\eta_k\cdot job_k^u\cdot\theta_k^u + \sum_{c\in C}\eta_c\cdot job_c^u\cdot\theta_c^u\\ & + \sum_{m\in M}\sum_{l\in L}\eta_m\cdot\mathrm{job}_m^{lu}\cdot\theta_m^{lu}\Big) + jt\times\sum_{r\in R}\sum_{u\in U}\sum_{t\in T}\Big(\sum_{p\in P}\sum_{g\in G}\frac{TP_r^g\cdot Q_{pr}^{gt}}{\mathrm{cap}_p^{gu}}\\ & + \sum_{p\in P}\sum_{k\in K}\frac{TK_r\cdot Q_{pkr}^t}{Cap_k^u} + \sum_{e\in E}\sum_{c\in C}\frac{TC_r\cdot Q_{ecr}^t}{Cap_c^u} + \sum_{c\in C}\sum_{m\in M}\sum_{a\in A}\sum_{l\in L}\frac{TM_a^l\cdot\rho_{ar}\cdot Q_{cmr}^t}{cap_m^{lu}}\Big),\end{aligned} \tag{14}$$

$$\mathrm{LD} = \sum_{u\in U}\Big(\sum_{p\in P}\sum_{g\in G} ltc_p^{gu}\cdot\theta_p^{gu} + \sum_{k\in K} ltc_k^u\cdot\theta_k^u + \sum_{c\in C} ltc_c^u\cdot\theta_c^u\sum_{m\in M}\sum_{l\in L} ltc_m^{lu}\cdot\theta_m^{lu}\Big)$$

$$+ lt \times \sum_{r\in R}\sum_{u\in U}\sum_{t\in T}\Bigg(\sum_{p\in P}\sum_{g\in G}\frac{TP_r^g \cdot Q_{pr}^{gt}}{cap_p^{gu}} + \sum_{p\in P}\sum_{k\in K}\frac{TK_r \cdot Q_{pkr}^t}{Cap_k^u}$$
$$+ \sum_{e\in E}\sum_{c\in C}\frac{TC_r \cdot Q_{ecr}^t}{Cap_c^u} + \sum_{c\in C}\sum_{m\in M}\sum_{a\in A}\sum_{l\in L}\frac{TM_a^l \cdot \rho_{ar} \cdot Q_{cmr}^t}{cap_m^{lu}}\Bigg). \tag{15}$$

Reliability Objective

This paper aims to model and evaluate the reliability of the supply chain in a fixed and variable manner. Potential suppliers and facilities have their reliability, which if selected and constructed, contributes to the overall reliability of the fixed part of the supply chain. The variable part of supply chain reliability comes from operational and transportation processes. The transportation of raw materials and distribution of products are subject to random failures. According to the studies of Fazli-Khalaf et al. [17], the reliability of the supply chain's variable part (operational reliability) is assumed to follow an exponential distribution with rate λ. Therefore, the component's reliability is equal to the probability expressed in Equation (16).

$$R_n = P(T_n > t) = e^{-\lambda_n t}; \quad \forall n = 1, 2, \cdots, N. \tag{16}$$

The product of the high probability multiplied by the number of products shipped from each potential facility to its next level is the number of products that arrive at their destination on time. Since the failure rate of transport routes and vehicles $(\lambda_{(x,y)} + \lambda_v)$ is considered per kilometer traveled, the product of the high probability (the sum of the failure rate of the route and vehicle) in the relevant distance, determines the reliability of transportation in the supply chain, which evaluates the responsiveness of the network, and the level of customer satisfaction. In addition, vehicle reliability measurement has not been considered in any SCND studies. Equation (17) maximizes supply chain reliability. Equation (18) calculates the reliability of the procurement process by considering suppliers' ability to meet manufacturers' needs as a reliable procurement process. Equation (19) calculates the possibility of establishing reliable potential facilities. Equation (20) calculates the reliability of operational activities. Equation (21) calculates the shipment reliability.

$$\text{Maximize} \quad Z3 = \text{Reliability} = \lambda_1 \times [\text{Contract Reliability (CR)}]$$
$$+ \lambda_2 \times [\text{Facility Reliability (FR)}] + \lambda_3 \times [\text{Operation Reliability (OR)}]$$
$$+ \lambda_4 \times [\text{Shipping Reliability (SR)}] \tag{17}$$

$$\text{CR} = \sum_{n\in S}\sum_{a\in A}\sum_{t\in T}\text{SR}_{sa} \cdot \theta_{sa}^t, \tag{18}$$

$$\text{FR} = \sum_{u\in U}\Bigg[\sum_{n\in P}\sum_{g\in G} RP_n^{gu} \cdot \theta_n^{gu} + \sum_{n\in K} RK_n^u \cdot \theta_n^u + \sum_{n\in C}\text{RC}_n^u \cdot \theta_n^u$$
$$+ \sum_{n\in M}\sum_{l\in L} RM_n^{lu} \cdot \theta_n^{lu}\Bigg], \tag{19}$$

$$\text{OR} = \sum_{x\in P}\sum_{r\in R}\sum_{g\in G}\sum_{t\in T} e^{-\lambda_p^{gut} \cdot t} \cdot TP_r^g \cdot Q_{pr}^{gt} + \sum_{x\in P}\sum_{y\in K}\sum_{r\in R}\sum_{t\in T} e^{-\lambda_k^{ut} \cdot t} \cdot TK_r \cdot Q_{pkr}^t$$
$$+ \sum_{x\in E}\sum_{y\in C}\sum_{r\in R}\sum_{t\in T} e^{-\lambda_c^{ut} \cdot t} \cdot \text{TC}_r \cdot Q_{ecr}^t$$
$$+ \sum_{x\in C}\sum_{y\in M}\sum_{a\in A}\sum_{r\in R}\sum_{l\in L}\sum_{t\in T} e^{-\lambda_m^{lut} \cdot t} \cdot TM_a^l \cdot \rho_{ar} \cdot Q_{cmr}^t, \tag{20}$$

$$\mathrm{SR} = \sum_{(x,y)\in\Phi'\cup\Phi''} \sum_{v\in V}\sum_{t\in T} e^{-(\lambda_v+\lambda_{xy}\cdot D_{xy})}\cdot \pi_{xy}^{vt}. \tag{21}$$

The following constraints are categorized and briefly explained. Studying the model becomes more accessible with this procedure.

CO2 Emissions Constraint

Equation (22) determines the amount of CO2 emissions in the supply chain.

$$\begin{aligned}\mathrm{CO}_2^{\mathrm{CUR}} = &\sum_{u\in U}\Bigg[\sum_{p\in P}\sum_{g\in G} E_p^{gu}\cdot\theta_p^{gu} + \sum_{k\in K} E_k^u\cdot\theta_k^u + \sum_{c\in C} E_c^u\cdot\theta_c^u \\ &+ \sum_{m\in M}\sum_{l\in L} E_m^{lu}\cdot\theta_m^{lu}\Bigg] + \epsilon^j\cdot\Bigg[\sum_{r\in R}\sum_{t\in T}\Bigg(\sum_{p\in P}\sum_{g\in G} EP_r^g\cdot Q_{pr}^{gt} + \sum_{(x,y)\in\Phi_5} EK_r\cdot Q_{xyr}^t \\ &+ \sum_{(x,y)\in\Phi_6} EC_r\cdot Q_{xyr}^t + \sum_{(x,y)\in\Phi_7}\sum_{a\in A}\sum_{l\in L} EM_a^l\cdot\rho_{ar}\cdot Q_{xyr}^t + \sum_{(x,y)\in\Phi_8} EB_r\cdot Q_{xyr}^t \\ &+ \sum_{(x,y)\in\Phi_9} EF_r\cdot Q_{xyr}^t\Bigg)\Bigg] + \epsilon^l\cdot\Bigg[\sum_{v\in V}\sum_{t\in T}\Bigg(\sum_{(x,y)\in\Phi'}\sum_{a\in A} D_{xy}\pi_{xy}^{vt}(FU1_v \\ &+ (FU2_v W_a Q_{xya}^t))\Bigg) + \Bigg(\sum_{(x,y)\in\Phi''}\sum_{r\in R} D_{xy}\pi_{xy}^{vt}(FU1_v + (FU2_v W_r Q_{xyr}^t))\Bigg)\Bigg].\end{aligned} \tag{22}$$

Budget Constraint

Equation (23) determines the maximum budget for potential facility establishment.

$$\sum_{u\in U}\Bigg[\sum_{p\in P}\sum_{g\in G} F_p^{gu}\cdot\theta_p^{gu} + \sum_{k\in K} F_k^u\cdot\theta_k^u + \sum_{c\in C} F_c^u\cdot\theta_c^u + \sum_{m\in M}\sum l\in LF_m^{lu}\cdot\theta_m^{lu}\Bigg] \leq \text{Budget}. \tag{23}$$

Demand Constraint

Equation (24) indicates that the lack of product in any period is equal to the difference between the actual demand and the delivery quantity to the market.

$$S_{er}^t = \mathrm{Dem}_{er}^t - \sum_{k\in K} Q_{\mathrm{ker}}^t, \quad \forall e, r, t. \tag{24}$$

Allocation Constraints

Equations (25), (26), (27), and (28) state that each manufacturing center, distribution center, collection center, and recycling center, respectively if established, can only have one capacity level.

$$\sum_{g\in G}\sum_{u\in U}\theta_p^{gu}\leq 1, \qquad \forall p \tag{25}$$
$$\sum_{u\in U}\theta_k^{u}\leq 1, \qquad \forall k \tag{26}$$
$$\sum_{u\in U}\theta_c^{u}\leq 1, \qquad \forall c \tag{27}$$
$$\sum_{l\in L}\sum_{u\in U}\theta_m^{lu}\leq 1, \qquad \forall m. \tag{28}$$

Facility Capacity Constraints

The minimum and maximum supplier capacities are shown by Equations (29) and (30), respectively. The maximum capacity of the manufacturing center is depicted by Equation (31). Equations (32) and (33) illustrate the distribution center's maximum distribution capacity and warehouse capacity, respectively. Equation (34) represents the maximum collection centers' collection capacity. The maximum recycling capacity of raw materials in the recycling center is described by Equation (35). Equation (36) shows the energy recovery center's maximum capacity and the maximum capacity of the landfill center is displayed by Equations (37).

$$\sum_{p\in P}Q_{spa}^t\geq b_{sa}\cdot\theta_{sa}^t, \qquad \forall s,a,t \tag{29}$$
$$\sum_{p\in P}Q_{spa}^t\leq \text{Cap}_{sa}\cdot\theta_{sa}^t, \qquad \forall s,a,t \tag{30}$$
$$\sum_{r\in R}\text{TP}_r^g\cdot Q_{pr}^{gt}\leq\sum_{u\in U}Cap_p^{gu}\cdot\theta_p^{gu}, \qquad \forall p,g,t \tag{31}$$
$$\sum_{e\in E}\sum_{r\in R}\text{TK}_r\cdot Q_{\text{ker}}^t\leq\sum_{u\in U}\text{Cap}_k^u\cdot\theta_k^u, \qquad \forall k,t \tag{32}$$
$$\sum_{r\in R}v_r\cdot I_{kr}^t\leq\sum_{u\in U}\text{VCap}_k^u\cdot\theta_k^u, \qquad \forall k,t \tag{33}$$
$$\sum_{e\in E}\sum_{r\in R}\text{TC}_r\cdot Q_{ecr}^t\leq\sum_{u\in U}\text{Cap}_c^u\cdot\theta_c^u, \qquad \forall c,t \tag{34}$$
$$\sum_{l\in L}\text{TM}_a^l\cdot\rho_{ar}\cdot Q_{cmr}^t\leq\sum_{l}\in L\sum_{u\in U}\text{Cap}_m^{lu}\cdot\theta_m^{lu}, \qquad \forall m,t \tag{35}$$
$$\sum_{c\in C}Q_{cbr}^t\leq\text{Cap}_{br}, \qquad \forall b,r,t \tag{36}$$
$$\sum_{c\in C}Q_{cfr}^t\leq\text{Cap}_{fr}, \qquad \forall f,r,t. \tag{37}$$

Flow Balance Constraints

Equation (38) does not allow for storage for the final products. Equation (39) shows manufacturing centers can obtain the raw materials they need by purchasing from suppliers or recycling centers. Equation (40) displays the maintenance quantity of final products in the distribution center. Equation (41) shows that the inventory of final products at the beginning of the first planning period is zero. Equation (42) shows the maximum storage time of final products in the warehouse is one period less than the end of their life. Equations (43) and (44) show the divided rate of recycled raw materials between the manufacturer and the secondary market, respectively. Equation (45) indicates that the return rate of end-of-life products (uptrend) depends on the time used. Equation (46) shows that final products do not return before their end of life. Equation (47) shows that the reverse chain may not collect all returned products from the primary market. Equation (48) displays the uncollected returned products. Equations (49), (50), and (51) show divide collected end-of-life products into three centers: energy recovery, recycling, and landfill, respectively.

$$\sum_{g\in G} Q_{pr}^{gt} = \sum_{k\in K} Q_{pkr}^{t}, \quad \forall p, r, t, \tag{38}$$

$$\sum_{s\in S} Q_{spa}^{t} + \sum_{m\in M} Q_{mpa}^{t} = \sum_{r\in R}\sum_{g\in G} q_{ar}\cdot Q_{pr}^{gt}, \quad \forall p, a, t, \tag{39}$$

$$I_{kr}^{t} = I_{kr}^{t-1} + \sum_{p\in P} Q_{pkr}^{t} - \sum_{e\in E} Q_{\text{ker}}^{t}, \quad \forall k, r, t, \tag{40}$$

$$I_{kr}^{t} = 0, \quad \forall k, r, t = 1, \tag{41}$$

$$\sum_{e\in E}\sum_{d=t}^{\min(t+D_r-1,T)} Q_{\text{ker}}^{d} - \sum_{p\in P}\sum_{t\in T} Q_{pkr}^{t} \geq 0, \quad \forall k, r, t, t\neq T, \tag{42}$$

$$\sum_{p\in P} Q_{mpa}^{t} = \sum_{c\in C}\sum_{r\in R} \sigma_a\cdot\rho_{ar}\cdot Q_{cmr}^{t}, \quad \forall m, a, t, \tag{43}$$

$$\sum_{h\in H} Q_{mha}^{t} = \sum_{c\in C}\sum_{r\in R} (1-\sigma_a)\cdot\rho_{ar}\cdot Q_{cmr}^{t}, \quad \forall m, a, t, \tag{44}$$

$$\text{QR}_{er}^{t} = \sum_{d=0}^{D_r} \omega_r^{d}\cdot(\text{Dem}_{er}^{t-d} - S_{er}^{t-d}), \quad \forall e, r, t, t\geq D_r, \tag{45}$$

$$\text{QR}_{er}^{t} = 0, \quad \forall e, r, t, t < D_r, \tag{46}$$

$$\sum_{c\in C} Q_{ecr}^{t} \leq \text{QR}_{er}^{t}, \quad \forall e, r, t, \tag{47}$$

$$\text{QN}_{er}^{t} = \text{QR}_{er}^{t} - \sum_{c\in C} Q_{ecr}^{t}, \qquad \forall e, r, t, \tag{48}$$

$$\sum_{e\in E} \beta_r\cdot Q_{ecr}^{t} = \sum_{b\in B} Q_{cbr}^{t}, \qquad \forall c, r, t, \tag{49}$$

$$\sum_{e\in E} \gamma_r\cdot Q_{ecr}^{t} = \sum_{m\in M} Q_{cmr}^{t}, \qquad \forall c, r, t, \tag{50}$$

$$\sum_{e\in E} Q_{ecr}^{t} = \sum_{m\in M} Q_{cmr}^{t} + \sum_{b\in B} Q_{cbr}^{t} + \sum_{f\in F} Q_{cfr}^{t}, \qquad \forall c, r, t. \tag{51}$$

Capacity Constraints for Shipments

Equations (52) and (53) represent the volume capacity of vehicles, while Equations (54) and (55) represent the weight capacity of vehicles.

$$\sum_{a\in A} v_a\cdot Q_{xya}^{t} \leq vcap^{v}\cdot\pi_{xy}^{vt}, \qquad \forall (x,y)\in\Phi', v, t, \tag{52}$$

$$\sum_{r\in R} v_r\cdot Q_{xyr}^{t} \leq vcap^{v}\cdot\pi_{xy}^{vt}, \qquad \forall (x,y)\in\Phi'', v, t, \tag{53}$$

$$\sum_{a\in A} w_a\cdot Q_{xya}^{t} \leq wcap^{v}\cdot\pi_{xy}^{vt}, \qquad \forall (x,y)\in\Phi', v, t, \tag{54}$$

$$\sum_{r\in R} w_r \cdot Q^t_{xyr} \le wcap^v \cdot \pi^{vt}_{xy}, \qquad \forall (x,y)\in \Phi^{''}, v, t. \tag{55}$$

Logical Constraints

Equations (56) and (57) provide logical constraints for both discrete and continuous decision variables.

$$\theta^t_{sa}, \theta^{gu}_p, \theta^u_k, \theta^u_c, \theta^{lu}_m, \pi^{vt}_{xy} \in \{0,1\}, \tag{56}$$
$$Q^{vt}_{xya}, Q^{vt}_{xyr}, Q^{gt}_{pr}, I^t_{kr}, QR^t_{xr}, QN^t_{er}, S^t_{er}, \mathrm{CO}_2^{CUR} \ge 0. \tag{57}$$

3.3.4 Linearization of the model

The model becomes non-linear due to multiplication relations between binary and positive variables in Equations (6) and (12) related to the first objective function, as well as Equation (22) related to the CO2 emissions constraint. Solving non-linear models is more complex than linear models [8]. Therefore, two new decision variables were defined to linearize the model, which replaces the nonlinear terms (see Table 3). The linearized equations are added to the model as Equations (58) to (65) are added to the model.

Table 3: Decision variables for linearization of the model.

Symbol	Description
SS^{vt}_{xya}	The amount of raw materials a transported by vehicle v between facilities $(x,y)\in\Phi^{'}$ in period t
SS^{vt}_{xyr}	The amount of product r transported by vehicle v between facilities $(x,y)\in\Phi^{''}$ in period t

Table 3 defines the symbols used for the decision variables. After linearization, Equation (6) becomes Equation (58), and Equations (12) and (22) become Equation (59). The new decision variables are subject to constraint Equation (66).

$$\begin{aligned}\mathrm{SC} = \sum_{v\in V}\sum_{t\in T}\Bigg[&\sum_{(x,y)\in\Phi^{'}}\sum_{a\in A} FU1_v\cdot V^t_v\cdot D_{xy}\cdot\pi^{vt}_{xy} + FU2_v\cdot V^t_v\cdot W_a\cdot D_{xy}\cdot SS^{vt}_{xya} + \frac{F^t_d\cdot D_{xy}\cdot\pi^{vt}_{xy}}{V^v}\Bigg]\\ &+\Bigg[\sum_{(x,y)\in\Phi^{''}}\sum_{r\in R} FU1_v\cdot V^t_v\cdot D_{xy}\cdot\pi^{vt}_{xy} + FU2_v\cdot V^t_v\cdot W_r\cdot D_{xy}\cdot SS^{vt}_{xyr} + \frac{F^t_d\cdot D_{xy}\cdot\pi^{vt}_{xy}}{V^v}\Bigg],\end{aligned} \tag{58}$$

$$\begin{aligned}\mathrm{CES} = \sum_{v\in V}\sum_{t\in T}\Bigg[&\sum_{(x,y)\in\Phi^{'}}\sum_{a\in A} FU1_v\cdot D_{xy}\cdot\pi^{vt}_{xy} + FU2_v\cdot W_a\cdot D_{xy}\cdot SS^{vt}_{xya}\Bigg]\\ &+\Bigg[\sum_{(x,y)\in\Phi^{''}}\sum_{r\in R} FU1_v\cdot D_{xy}\cdot\pi^{vt}_{xy} + FU2_v\cdot W_r\cdot D_{xy}\cdot SS^{vt}_{xyr}\Bigg],\end{aligned} \tag{59}$$

$$SS^{vt}_{xya} \le Q^t_{xya}, \qquad \forall (x,y)\in\Phi^{'}, a, v, t, \tag{60}$$
$$SS^{vt}_{xya} \le BM\cdot\pi^{vt}_{xy}, \qquad \forall (x,y)\in\Phi^{'}, a, v, t, \tag{61}$$
$$SS^{vt}_{xya} \ge Q^t_{xya} - BM\cdot(1-\pi^{vt}_{xy}), \qquad \forall (x,y)\in\Phi^{'}, a, v, t, \tag{62}$$
$$SS^{vt}_{xyr} \le Q^t_{xyr}, \qquad \forall (x,y)\in\Phi^{''}, r, v, t, \tag{63}$$

$$SS_{xyr}^{vt} \leq BM \cdot \pi_{xy}^{vt}, \qquad \forall (x,y) \in \Phi^{''}, r, v, t, \tag{64}$$

$$SS_{xyr}^{vt} \geq Q_{xyr}^{t} - BM \cdot (1 - \pi_{xy}^{vt}), \qquad \forall (x,y) \in \Phi^{''}, r, v, t, \tag{65}$$

$$SS_{xya}^{vt}, SS_{xyr}^{vt} \geq 0. \tag{66}$$

3.4 Model solving

Within this section, we will provide an explanation of various methods for solving the problem.

3.4.1 The AEC method

In the AEC method, the results of individual optimization of objective functions to complete the Payoff table (range of ε values) are calculated using lexicographic optimization. Additionally, the constraints of the objective functions are converted to equality by introducing appropriate auxiliary variables. This second-order term in the objective function, with lower priority than the lexicographic method, forces the model to produce only Pareto solutions [35]. If the problem is infeasible, the solution algorithm stops and is not solved for subsequent iterations, which increases the solution speed compared to the conventional ε-constraint method. There is a trade-off between the number of Pareto solutions generated and the solve time, and the density of the Pareto collection can be controlled. According to the original ε-constraint method, one objective of the problem is optimized according to the decision maker's priority, while the other objectives are limited to the upper limit of ε. The resulting equation is Equation (67).

$$\begin{cases} \text{Max} \quad F_1(x) - \delta \times \left[\frac{s_2}{r_2} + (10^{-1} \times \frac{s_3}{r_3}) + \cdots + (10^{-(n-2)} \times \frac{s_n}{r_n}\right] \\ \text{s.t :} \\ F_i(x) + s_i = e_i, \qquad i = 2, 3, \cdots, n, \quad x \in S, \quad s_i \in R^+, \end{cases} \tag{67}$$

where S represents the solution region of the model, e_i is the value to the right of the objective functions, and δ is a small number (usually $\delta \in [10^{-6}, 10^{-3}]$). r_i denotes the domain of the i-th objective function which is determined by table calculations. The model incorporates a form of lexicographic optimization in the second expression of the objective function to ensure the existence of another optimal solution for the remaining objectives. [35]. This approach allows the solver to find the best case for F_1 and subsequently optimize the other objectives in order.

3.4.2 Normalized normal constraint (NNC)

Figure 3 displays the ultra-surface of the Pareto frontier for a three-objective optimization problem, where the ultra-surface takes the form of a 3D objective space. The NNC method is an exact solution approach that yields a set of Pareto optimal points rather than a unique optimal point for multi-objective problems [3]. Compared to the ε-constraint (EC) method [34], the NNC method offers more advantageous features. In the NNC method, the objectives are first normalized and then new constraints are applied in each phase to search for optimal solutions. The NNC method has been proven to effectively solve multi-objective SCND problems in previous studies [6, 21, 46]. Uniformly distributing the solutions at the Pareto boundary facilitates decision-making for selecting the optimal solution. However, most techniques do not report well-distributed Pareto solutions [36]. The NNC method allows the density of Pareto sets to be controlled by a single parameter m_1, with other settings of m_2 to $m_{(n-1)}$ being automatically adjusted accordingly. This feature enhances the applicability and ease of implementation of the NNC method Increasing m_1 leads to a denser set of Pareto solutions but also incurs higher computational cost. Moreover, the NNC method does not require the determination of initial weights for the objectives [49].

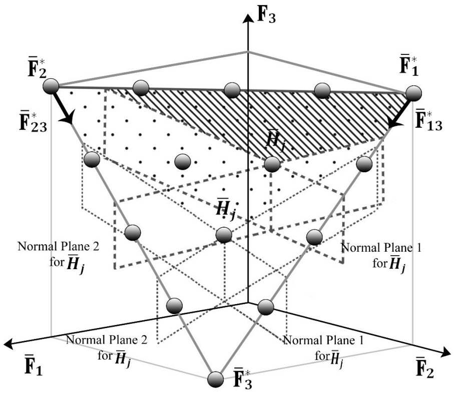

Figure 3: The NNC technique for a three-objective optimization problem.

The NNC method is a solution approach for multi-objective optimization problems includes involves the following process [41].

Step 1. The optimal objective function i is denoted by u^{i*}, and it is obtained by solving a single-objective problem using Equation (68). By utilizing the solutions u^{i*}, the anchor points f^{i*} are generated as Equation (69). A utopian world is then formed by connecting these anchor points in the objective space, called the ideal utopia.

Step 2. This Step involves normalizing targets that have varying and sometimes inconsistent scales to prevent them from influencing the optimization process. An ideal point, denoted as (f^u), represents the best solution regarding the objective function and is determined using Equation (70). The counter-point f^N represents the worst solution of the objective function and is calculated using Equation (71). Equation (72) is therefore applicable. Each objective function is normalized using Equation (73), where $\bar{f}_i$ represents the normalized form of f_i. In Figure 3, which depicts a three-objective optimization problem, the normalized objective functions $\bar{f}_1, \bar{f}_2$ and $\bar{f}_3$ are used to coordinate the target space with anchor points $\bar{f}^{1*}$, $\bar{f}^{2*}$ and $\bar{f}^{3*}$ also being normalized.

Step 3. The normalized ideal hyper-surface vectors ($\bar{N}_k$) are calculated using Equation (74). Each vector $\bar{N}_k$ is drawn directly from the normalized pillar point $k(\bar{f}^{k*})$ to the normalized pillar point $nm(\bar{f}^{n*})$. Figure 3 illustrates the vector way of $\bar{N}_1$ from $\bar{f}^{1*}$ to $\bar{f}^{3*}$ and the way $\bar{N}_2$ from $\bar{f}^{2*}$ to $\bar{f}^{3*}$ is drawn.

Step 4. A normalized length (δ_k) is determined for a specific number of divisions (m_k) on the vector $\bar{N}_k$ using Equation (75). In the NNC method, each m_k is consistent to with m_1 is calculate as per Equation (76).

Step 5. involves obtaining the wonderland hyperspace points $(\bar{X}_j)$ in achieved on the normalized wonderland hyperspace using Equation (77)), where the coefficients $\alpha_{kj}(k = 1, \cdots, k = n-1)$; $\sum_{k=1}^{n} \alpha_{kj=1}$ and $0 \leq \alpha_{kj} \leq 1$ are different. From the normalized increase of δ_k in Equation (74). The last coefficient α_{njis} equal to $\alpha_{nj} = 1 - \sum_{k=1}^{n-1} \alpha_{kj}$. For instance, in a three-objective optimization problem (i.e., $n = 3$) with $m1 = m2 = 5$, the values of $\alpha kj(k = 1, 2, 3)$ are shown in Figure 4, where $\delta_1 = \delta_2 = 0.25$. In this problem, 15 optimal $\bar{X}_j(1 \leq j \leq 15)$ rays are obtained, which are represented by small black circles in Figure 3.

Step 6. involves determining the Pareto optimal point for each wonderland hyperspace point obtained by solving the one-objective optimization problem in Equation (78).

$$u^{i*} = \text{arg min}\, f_i(u)$$
$$\text{subject to : } \begin{cases} \phi(u) = 0 & i = 1, 2, \cdots, n, \\ \Phi(u) \leq 0, \end{cases} \tag{68}$$

$$\begin{aligned} f^{i*} &= \left[f_1^{i*} \quad f_2^{i*} \quad \cdots \quad f_n^{i*}\right]^T, \quad i = 1, 2, \cdots, n \\ &= \left[f_1(u^{i*}) \quad f_2(u^{i*}) \quad \cdots \quad f_n(u^{i*})\right]^T, \quad i = 1, 2, \cdots, n, \end{aligned} \tag{69}$$

$$f^u = \left[f_1^u \quad f_2^u \quad \cdots \quad f_n^u\right]^T = \left[f_1(u^{1*}) \quad f_2(u^{2*}) \quad \cdots \quad f_n(u^{n*})\right]^T, \tag{70}$$

$$f^N = \left[f_1^N \quad f_2^N \quad \cdots \quad f_n^N\right]^T, \tag{71}$$

$$f_i^N = \max\{f_i(u^{1*})\, f_i(u^{2*}) \cdots f_i(u^{n*})\}, \quad i = 1, 2, \cdots, n, \tag{72}$$

$$\bar{f}_i = \frac{f_i - f_i^U}{f_i^N - f_i^U}, \quad i = 1, 2, \cdots, n, \tag{73}$$

$$\bar{N}_k = \bar{f}^{n*} - \bar{f}^{k*}, \quad k = 1, 2, \cdots, n-1, \tag{74}$$

$$\delta_k = \frac{1}{m_k - 1}, \quad k = 1, 2, \cdots, n-1 \tag{75}$$

$$\frac{m_k}{\|\bar{N}_k\|} = \frac{m_1}{\|\bar{N}_1\|}, k = 1, 2, \cdots, n-1, \tag{76}$$

$$\bar{X}_j = \sum_{k=1}^{n} \alpha_{kj} \cdot \bar{f}^{k*}. \tag{77}$$

$$\begin{aligned} &\min \quad \bar{f}_n(u) \\ &\phi(u) = 0, \quad \phi(u) \leq 0, \\ &\bar{N}_k \cdot (\bar{f} - \bar{X}_j) \leq 0, \quad k = 1, 2, \cdots, n-1, \\ &\bar{f} = [\bar{f}_1(u), \bar{f}_1(u), \cdots, \bar{f}_n(u)]^T. \end{aligned} \tag{78}$$

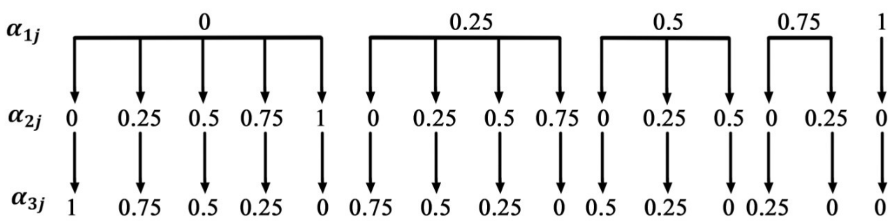

Figure 4: Coefficients for a three-objective problem with $m1 = m2 = 5$.

3.4.3 Shannon entropy technique

The Shannon entropy technique was utilized in this study to determine the relative importance of appraisal criteria. This technique is widely used for calculating the criteria weights [30]. The entropy technique utilizes decision matrix information to assign weight to the criteria, with more weight given to the index that creates greater differentiation between the options. Equations (79) to (84) were used to implement the Shannon entropy process.

$$X = [x_{ij}]_{n \times m} = \begin{bmatrix} x_{11} & x_{12} & \cdots & x_{1m} \\ x_{21} & x_{22} & \cdots & x_{2m} \\ \ddots & \ddots & \ddots & \ddots \\ x_{n1} & x_{n2} & \cdots & x_{nm} \end{bmatrix}, \tag{79}$$

$$P_{ij} = \frac{r_{ij}}{\sum_{i=1}^{m} r_{ij}}, \quad \forall i, j, \tag{80}$$

$$E_j = -k \sum_{i=1}^{m} [P_{ij} \times LnP_{ij}], \quad \forall j, \tag{81}$$

$$k = \frac{1}{Lnm}, \tag{82}$$

$$d_j = 1 - E_j, \qquad \forall j, \tag{83}$$

$$w_j = \frac{d_j}{\sum_{j=1}^{n} d_j}, \quad \forall j. \tag{84}$$

Equation (79) represents the decision matrix for both the AEC and NNC methods, where the rows and columns represent the options and indicators, respectively. For example, the x_{12} array shows the score of the first alternative relative to the second criterion. The normal decision matrix is obtained by dividing each column's value by the sum of that column, as shown in Equation (80), where P_{ij} specifies normalized data. The entropy of each criterion is calculated using Equation (81), where k is a constant value ensuring that $0 \leq E_j \leq 1$. The value of k is determined using Equation (82). The degree of deviation (d_j) is calculated using Equation (83), which provides information for the decision maker to decide. A smaller value of d_j indicates that the criterion does not make much difference between competing alternatives and hence should be less important in decision-making. Finally, Equation (84) is used to calculate the weight of each criterion.

3.4.4 VIKOR technique

Once the weight of each criterion has been determined, the next step is to evaluate the alternatives. In this study, the VIKOR technique was used to evaluate the alternatives using the AEC and NNC methods, VIKOR is a multi-criteria optimization technique that was proposed in 1984 by a Serbian researcher named Opricovic. This technique is particularly useful when decision-makers are faced with contradictory criteria that make it difficult for them to express their preferences. In these cases, the decision-makers can agree upon compromise solutions obtained from the VIKOR technique. This solution minimizes both group desirability (by the S criterion) and individual influences (by the R criterion) to the minimum. The first and second steps of the VIKOR technique involve forming a decision matrix and determining the weight of the criteria, respectively, as discussed in the previous section. The subsequent steps of this method are shown in Equations (85) to (90).

$$f^{+} = \max f_{ij}; \quad f^{-} = \min f_{ij}, \tag{85}$$

$$S_j = \sum_{i=1}^{n} w_i \cdot \frac{f_i^* - f_{ij}}{f_i^* - f_i^-}, \tag{86}$$

$$R_j = \max[w_i \cdot \frac{f_i^* - f_{ij}}{f_i^* - f_i^-}], \tag{87}$$

$$92Q_j = v \cdot \frac{S_j - S^*}{S^- - S^*} + (1 - v) \cdot \frac{R_j - R^*}{R^- - R^*}, \tag{88}$$

$$S^{-} = \max S_j, \quad S^* = \min S_j, \tag{89}$$

$$R^{-} = \max R_j, \quad R^{*} = \min R_j. \tag{90}$$

The third step involves determining the ideal positive and negative points, which are denoted by f^{+} and f^{-} respectively. These points are identified for criteria with a profit aspect in Equation (85), and the best and the worst of each criterion among the alternatives are used for this purpose. Equations (86) and (87) are used to calculate the usefulness S and the amount of regret R for each alternative, respectively. The relative distance of alternative j from the ideal solution (best combination) is determined by S_j, and R_j represents the maximum inconvenience of alternative j from the ideal point. These steps complete the fourth step. In the fifth step, the VIKOR index is calculated with the symbol Q_j using Equation (88), which takes into account the importance of group agreement (parameter v). A high group agreement is indicated by $v > 0.5$, while $v = 0.5$ represents group agreement with the majority vote, and $v < 0.5$ indicates low group agreement. Equation (89) and (90) represent the symbols S^{-} and S^{*}, R^{-} and R^{*}, respectively. In the sixth step, the alternatives are sorted based on descending values of the S, R, and Q indicators. The alternative with the lowest Q value is selected as the best alternative if it satisfies two conditions.

To determine the acceptability score of substitutes A_1 and A_2, Equation (91) must be established. First, if A_1 and A_2 are ranked first and second among the available alternatives, respectively.

$$(A_2) - Q(A_1) \geq \frac{1}{m-1}, \tag{91}$$

second, alternative A_1 must have reached the top rank in at least one of the S and R groups to ensure acceptable consistency in decision-making. If either of these conditions is not met, both substitutes are considered equally good or superior.

3.4.5 Evaluation criteria

In multi-objective optimization, preference is given over single-objective optimization. The aim is to determine the degree to which a solution satisfies various objectives. After generating Pareto optimal solutions, the most preferred point for the multi-objective optimization problem is selected based on the importance of each objective function. Equation (92) defines the Pareto optimal point of k, denoted by P_k,

$$P_k = \sum_{i=1}^{n} \left(IF_i \frac{f_i^N - f_{ki}}{f_i^N - f_i^U} \right), \tag{92}$$

where f_i^U and f_i^N are robust and weak efficiency solutions defined in Equations (70) and (71) respectively. Furthermore, f_{ki} represents the result obtained for the objective function i in k's Pareto optimal point. The essential coefficient of each objective function, denoted by IFi, is in the range of $[0, 1]$, and their sum equals one must specify essential coefficients. The Pareto optimal solution that optimizes more essential objective functions, i.e., whose f_{ki} results are closer to the consistent f_i^U values or has a value $(f_i^N - f_{ki}/f_i^N - f_i^U)$ closer to one is sanctioned as P_k, meaning that it is the sanctioned solution to the multi-objective optimization problem. Additionally, considering IFi in Equation (92) prioritizes Pareto optimal solution that optimizes more essential objective functions (i.e., with higher IFi values) a higher priority. The Pareto optimal solution with the highest P_k value is sanctioned and the final solution to the multi-objective optimization problem is chosen as the Pareto optimal solution with the highest P_k value.

The NNC method has only one property, m_1. In sensitivity analysis, m_1 is changed around its base value in both negative and positive directions with a step equal to the sensitivity coefficient calculated using Equation(93).

$$F(\%) = \frac{\Delta P_k}{\Delta m_1} \times 100 = \frac{\text{base } P_k - \text{deviated } P_k}{\text{base } m_1 - \text{deviated } m_1} \times 100. \tag{93}$$

In this study, the best solution for the three objective functions serves as the basis for further comparison. Given that the GAMS software yields the optimal solution for each objective function, the performance of solution methods is evaluated using the relative error percentage criterion, as calculated by Equation (94).

$$\text{PRE} = \frac{\text{Real}_{\text{solution}} - \text{Ideal}_{\text{solution}}}{\text{Ideal}_{\text{solution}}} \times 100, \tag{94}$$

the $\text{Real}_{\text{solution}}$ refers to the value of the objective function obtained through the method, while the $\text{Ideal}_{\text{solutionis}}$ represents the optimal value of the objective function, which was obtained by solving the complex integer model in GAMS software. A lower value of this criterion indicates a higher quality of responses.

Furthermore, the following section introduces and calculates the criteria for evaluating Pareto solutions, in addition to the initial comparisons that demonstrated the superior performance of the NNC method. The Run Time (RT), Mean Ideal Distance (MID), Diversification Metric (DM), and General Distance Metric (GDM) are used as the basis for evaluating the performance of AEC and NNC solutions methods in this study. The definition and calculation method for each criterion are as follows.

The Run Time (RT) is the time taken by each method to solve the problem and is one of the most essential bases for comparing multi-objective problem-solving methods. A better method has a shorter solving time, which is considered a negative aspect.

The Mean Ideal Distance (MID) measures the proximity of Pareto points to the ideal point. As all three objective functions of this research problem are of the maximization type, symbols $f_1^{\max}$, $f_2^{\max}$ and $f_3^{\max}$ represent the ideal points of the functions, respectively. Equation (95) outlines how to calculate MID.

$$\text{MID} = \frac{\sum_{i=1}^{n} \left\{ \left(\frac{f_{1,i} - f_1^{\max}}{f_{1,\text{total}}^{\max} - f_{1,\text{total}}^{\min}} \right)^2 + \left(\frac{f_{2,i} - f_2^{\max}}{f_{2,\text{total}}^{\max} - f_{2,\text{total}}^{\min}} \right)^2 + \left(\frac{f_{3,i} - f_3^{\max}}{f_{3,\text{total}}^{\max} - f_{3,\text{total}}^{\min}} \right)^2 \right\}^{\frac{1}{2}}}{n}. \tag{95}$$

Here, n represents the number of Pareto points, and the maximum and minimum values of the unsuccessful objective functions obtained in all model executions are denoted by $f_{i,\text{total}}^{\max}$ and $f_{i,\text{total}}^{\min}$, respectively. A lower MID value is considered a be tter method (negative aspect).

The Diversification Metric (DM) measures the extent of Pareto's solutions by calculating the Euclidean distance between the initial and final solutions of the Pareto set of solutions [53]. This criterion is calculated based on Equation (96), and a higher DM value is considered a better method (positive aspect).

$$\text{DM} = \sum_{i=1}^{n} \left\{ \left(\frac{\max f_{1,i} - \min f_{1,i}}{f_{1,\text{total}}^{\max} - f_{1,\text{total}}^{\min}} \right)^2 + \left(\frac{\max f_{2,i} - \min f_{2,i}}{f_{2,total}^{\max} - f_{2,\text{total}}^{\min}} \right)^2 + \left(\frac{\max f_{3,i} - \min f_{3,i}}{f_{3,\text{total}}^{\max} - f_{3,\text{total}}^{\min}} \right)^2 \right\}^{\frac{1}{2}}. \tag{96}$$

General Distance Metric (GDM) evaluates the uniformity of Pareto solution distribution in the solution space by considering the deviation of the distance criterion of efficient solutions. This criterion measures the relative distance of consecutive Pareto solutions [10]. The method of calculating this criterion is according to Equation (97).

$$\text{SM} = \sqrt{\frac{1}{n-1} \sum_{i=1}^{n} (d_i - \bar{d})^2}, \tag{97}$$

$$d_i =_j^{\min} \{|f_{1i} - f_{1j}| + |f_{2i} - f_{2j}| + |f_{3i} - f_{3j}|\}, \quad i, j = 1, 2, \ldots, n; i \neq j, \tag{98}$$

$$\bar{d} = \frac{\sum_{i=1}^{n} d_i}{n}. \tag{99}$$

Determining Pareto boundary points based on Equation (97) in three-dimensional space requires more complex calculations and time. Therefore, a straightforward relation is used to determine Pareto points' scattering (Equation (100)).

$$SM = \frac{\sum_{i=1}^{n} |\bar{d} - d_i|}{n \times \bar{d}}, \tag{100}$$

where, d_i indicates the number of Pareto points in cell i, and $\bar{d}$ is the average number of Pareto points in all cells. Accordingly, the cell solution space is divided into several specific areas (see Figure 5). Each of the three small three-dimensional cells in this diagram contains several Pareto points. A lower standard deviation of the distance between Pareto points in the created cells is considered a better method (negative aspect).

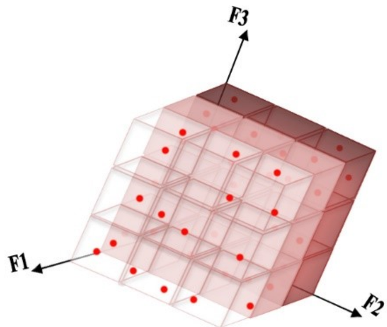

Figure 5: Cell configuration of the solution area and location of Pareto points in cells.

4 Results

This section presents a numerical example to solve the mathematical model discussed in the previous section. The numerical example comprises five suppliers, six manufacturers, four distributors, eight customers, four collection centers, six recycling centers, and four periods. Other experimental parameters are randomly generated through the uniform distribution function. In multi-objective problems, optimizing one objective function may lead to deterioration in the other objectives [40]. Thus, an outcome matrix is created for the goals to determine if there is a conflict between objectives. For this purpose, the other objectives are optimized individually while subject to their optimality, and the results are presented in Table 3 for the green profitability (f1), social responsibility (f2), and reliability (f3) functions. The results in Table 4 show that individual optimization of each objective function leads to acceptable outcomes for that objective function but unsuitable outcomes for the other objective functions. For instance, f2 = 1282.13 obtained from single-objective optimization of f3 is 0.27 less than f2 = 1756.73 obtained from single-objective optimization f2. Similarly, f3 = 2.96 obtained from single-objective optimization f1 is 0.4 less than f3 = 4.91 obtained from single-objective optimization f3. Therefore, single-objective optimization cannot provide a good compromise between rival objective functions highlighting the need for multi-objective optimization for the SCND problem.

In general, the mathematical model presented in this paper considers three objectives: economic profit, social responsibility, and reliability which may conflict with each other. To minimize purchasing costs, it may be beneficial to secure a raw material supply contract with a supplier offering lower prices. However, such a supplier may be located further away from the plant, resulting in increased carbon emissions and associated costs. To minimize the cost of carbon emissions, choosing a close supplier can

Table 4: Payoff Matrix of objectives for little size problem.

Consequences	Objective 1	Objective 2	Objective 3
Profitability optimization (f1)	14465372.18	1531.84	2.96
social responsibility optimization (f2)	13916527.04	1756.73	4.24
Reliability optimization (f3)	12296024.95	1282.13	4.91

be beneficial. However, their reliability may be compromised due to limited access to energy sources, which are often closer to distant suppliers. Additionally, the purchase price of materials may be higher than that of other suppliers. Therefore, decision-makers must weigh the benefits of each objective and make a trade-off between them. To illustrate the proposed approach, four different examples are considered based on the significant coefficients of the objective functions f1, f2, and f3, as shown in Table 5. IZ1, IZ2, and IZ3 show represent the significant coefficients of the functions f1, f2, and f3, respectively.

Table 5: Different samples of the designed experimental example.

Sample counter	Objective		
	IZ1	IZ2	IZ3
First	0.33	0.33	0.33
Second	0.25	0.25	0.5
Third	0.25	0.5	0.25
Fourth	0.5	0.25	0.25

In practice, the company's management can determine the importance of the coefficients based on the technical and economic conditions of the industry they operate in. In the first sample, the same importance is assigned to the objectives with a coefficient of 0.33 for each. In the second case, social responsibility and reliability are considered equally important, with coefficients of 0.25 each. Profitability with a coefficient of 0.5 is considered more essential because all businesses generally aim to make a profit. With this approach, the third model places more emphasis on social responsibility, while the fourth places more emphasis on reliability. As stakeholders often monitor corporate social responsibility, in addition to its real-world applications, a supply chain's reliability may be more vulnerable to its profitability or social responsibility.

The proposed sustainable and reliable SCND problem (relationships 1 to 60) was solved using multi-objective problem-solving methods and compared with AEC and NNC techniques. To solve the example, both AEC and NNC methods were implemented in the GAMS 24.2.1 software package using the CPLEX solver. These results are presented in normalized form for the four samples in Table 6. To ensure a fair comparison, both solving methods generated 66 Pareto solutions. The NNC method used $m_1 = 11$ to generate 66 Pareto solutions, while the AEC method determined the appropriate step for ε to achieve the desired Pareto number. Due to the nonlinear and multi-objective (three objective functions) nature of the proposed SCND model, the problem is NP-hard and requires considerable time to solve. The calculation times of the NNC and AEC methods are approximately 1633 and 2465 seconds, respectively, measured on an Intel Core i7 laptop with a 2.4 GHz processor and 16 GB of memory. The NNC's shorter computing time is a crucial advantage, facilitating its practical application to solve the multi-objective problem in SCND.

The NNC and AEC methods produce a set of Pareto optimal points and select the best solution. The results of Table 5 show that the AEC method is better than the NNC only in the third sample, but the NNC outperforms the AEC in searching the Pareto border more effectively. To illustrate this feature, the Pareto set produced by the NNC is compared to that produced by the AEC in Figure 6.

Table 6: Obtained results for the four experimental samples.

Normalized objective	Technique	Normalized objective			Pk
		$\bar{f}_3$	$\bar{f}_2$	$\bar{f}_1$	
First	NNC	0.217	0.171	0.301	0.7702
	AEC	0.018	0.149	0.558	0.7585
Second	NNC	0.201	0.169	0.327	0.7755
	AEC	0.021	0.168	0.751	0.7597
Third	NNC	0.236	0.146	0.314	0.7895
	AEC	0.019	0.138	0.544	0.7902
Fourth	NNC	0.231	0.168	0.355	0.7227
	AEC	0.020	0.132	0.545	0.6895

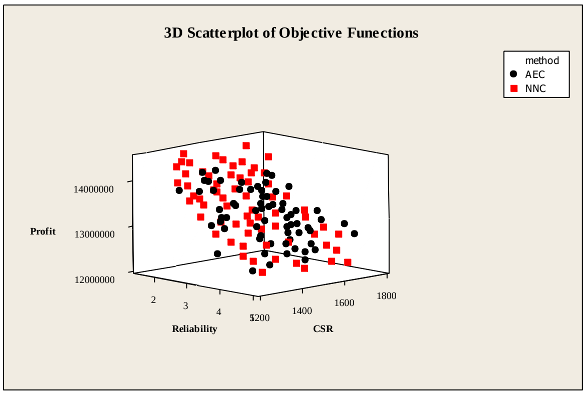

Figure 6: Efficient solutions obtained by AEC and NNC methods.

This figure shows that the NNC method can search for areas of the Pareto border that the AEC method does not have to access. Therefore, the NNC can be more suitable for covering the Pareto border than the AEC. Additionally, it is observed that the preferred NNC solutions differ from the preferred AEC solutions because the most preferred NNC solutions are located in parts of the Pareto boundary that only the NNC can search (such as some edges of the Pareto boundary).

Table 6 performed a sensitivity analysis of the NNC method by setting m_1 to values that differed from its base value (11) in both negative and positive directions with a step equal to two. Values $11-2\times 3 = 5$ (three-step of negative), $11 - 2 \times 2 = 7$ (two-step of negative), 11 - 2 = 9 (one-step of negative), 11 (without deviation), 11 + 2 = 13 (one-step of positive), $11 + 2 \times 2 = 15$ (two-step of positive), and $11+2\times 3 = 17$ (three-step of positive) are considered for setting m_1 . For each m_1 value, the number of Pareto points, the values of the objective functions f_1, f_2, and f_3, the P_k preference, and the sensitivity coefficient (SF) percentage are shown in Table 7.

Table 6 indicates that the P_k preference changes slightly by altering the m_1 setting, resulting in low sensitivity coefficient values and demonstrating the stability of the NNC method. The only weak result for the NNC method is the lower P_k in the third sample compared to the AEC method. However, this difference is only 0.0007, while in the first sample (0.0117), in the second sample (0.0158), and in the fourth sample (0.0332), this difference is in favor of the NNC method. Table 8 shows the PRE values for all three objective functions in the AEC and NNC methods. Carefully, examining the table information, it can be inferred that in the first and second objective functions, the NNC method has less deviation

Table 7: The results of sensitivity analysis on the setting m_1 in the first case.

m_1	No. Pareto solution	Normalized objectives			Pk	SF
		$\bar{f}_1$	$\bar{f}_2$	$\bar{f}_3$		
5	15	0.213201	0.183069	0.308227	0.765402	0.081183
7	28	0.201151	0.175092	0.320135	0.768106	0.054175
9	45	0.186021	0.195018	0.309151	0.770167	0.005300
11	66	0.217301	0.171325	0.301245	0.770273	0
13	91	0.187099	0.190684	0.310719	0.770729	0.022800
15	120	0.190144	0.174962	0.322183	0.771133	0.021500
17	153	0.210987	0.197281	0.248304	0.781362	0.184816

from the optimal state than the AEC method. Additionally, compared to the NNC method, the AEC method can estimate the value of the third objective function with less deviation from the ideal situation.

Table 8: Percentage of relative error (PRE) for solving methods.

Solving method	Objectives		
	f_1	f_2	f_3
AEC	2.16616	25.4133	33.6396
NNC	1.65093	10.6366	54.4292

The decision matrix is presented in Table 9. This table includes the values of each index in the AEC and NNC methods. Table 10 presents the criteria weights based on Shannon's entropy method. The results of the comparison and ranking of AEC and NNC methods in solving research problems using the VIKOR technique are presented in Table 11. The superiority of the NNC method over the AEC method is demonstrated by the information in the table.

Table 9: Final decision matrix.

	$\overset{-}{RT}$	$\overset{-}{MID}$	$\overset{+}{DM}$	$\overset{-}{SM}$
AEC	2465	1.030707	1.964588	1.141415
NNC	1633	1.260091	2.233026	0.787879

Table 10: Attributes weighting with Shanon entropy technique.

Symbol	Title	Criteria			
		RT	MID	DM	SM
E_j	Entropy	0.970059	0.992755	0.997048	0.97564
d_j	Degree of deviation	0.029941	0.007245	0.002952	0.02436
w_j	Normalized weight	0.464222	0.112326	0.04577	0.377682

Table 11: Results of comparison of AEC and NNC methods.

Method	S	R	Q	Rank
AEC	0.887674	0.464222	1	Second
NNC	0.112326	0.112326	0	First

5 Discussion

5.1 Sensitivity analysis of mathematical model

To validate and examine the behavior of the proposed model more accurately, the sensitivity of the parameters to changes in their value is observed. Therefore, in this section, by changing the demand in the primary market (Dem_{er}^{t})), the behavior of the model's three objective functions, profit, social responsibility, and reliability, is examined. The effect of changing the value of objective functions, including profitability, social responsibility, and reliability, under the influence of the primary market demand parameter (Dem_{er}^{t}) is shown in Figure 7. This Figure shows that profitability increased with an increase in primary market demand, but social responsibility and reliability decreased. Given the cost of fines for shortages, the model tries to satisfy the maximum demand. The operational strategy of production management is to increase production when faced with a sudden increase in customer demand. This strategy is expressed in the profitability objective function of the mathematical model by multiplying the selling price of products and production costs (parameter) by the number of production, which is a decision variable.

The proposed model suggests that the level of supply chain social responsibility is influenced by the number of production, but it has a negative impact. Increasing production to meet rising demand often results in overworking existing staff instead of hiring new employees. Moreover, maximizing nominal production capacity by increasing working hours can result in increased sick leave usage among employees. Consequently, an increase in demand can lead to decreased social responsibility and increased reliability, as illustrated in Figure 6. This can be attributed to the fact that meeting higher demand requires more raw materials, which may necessitate contracting with less reliable suppliers. Given that suppliers' capacity is limited, it is often impossible for a single supplier to meet the supply chain's needs under normal circumstances, and this problem is further exacerbated by increasing demand. In terms of supply chain design, customer satisfaction is typically prioritized over reliability.

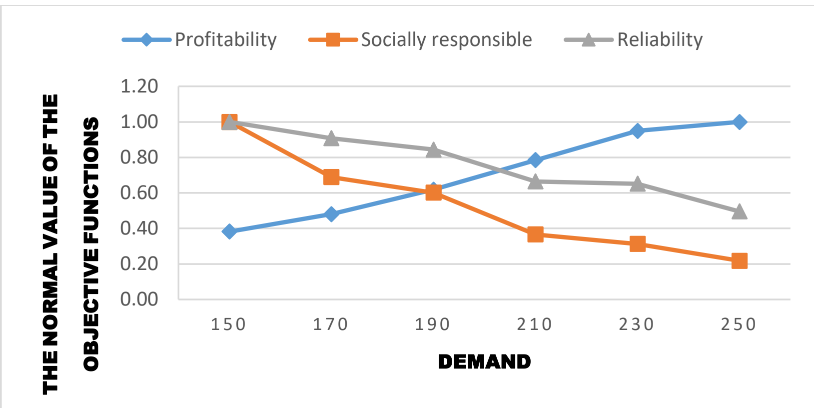

Figure 7: Sensitivity analysis of changes in demand.

5.2 Sensitivity analysis of the solution method

This section aims to validate and analyze the sensitivity of the problem model's solution methods. Intended sensitivity analysis examines the variability of the proposed ranking by changing the criteria weights. To this end, the ranking of alternatives after assigning equal weight to the criteria is compared with the initial ranking. In this regard, the alternatives' usefulness, regret, and VIKOR index values are shown with the weights obtained from the Shannon entropy method for the criteria in Part A of Figure 8 and equal weights for the criteria in Part B of Figure 8. These values play a crucial role in ranking alternatives in the VIKOR process. In Figure 8, it can be concluded that even with the same importance assigned to the criteria, the ranking result has not changed. This result emphasizes the desirability and priority of the NNC method in different situations.

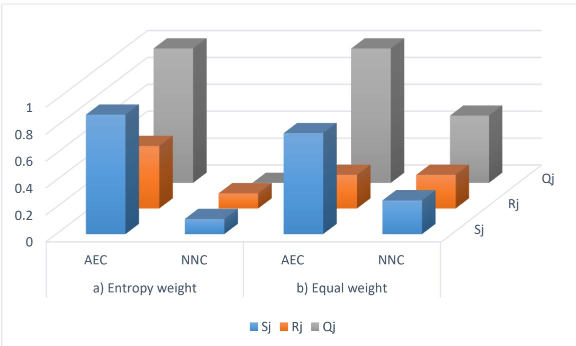

Figure 8: The effect of attribute weighting on alternative ranking (a: Shannon entropy weights - b: equal weights).

The criteria used in both AEC and NNC methods, as presented in Figure 9, can be compared to determine the reasons for the superiority and strengths of one method over the other. Therefore, the superiority of the NNC technique compared to the AEC method can be attributed to the criteria of run time, diversification metric, and standard deviation metric. A comparison of the length between the solutions and the optimal solution in the AEC and NNC methods reveals that the length between the points and the ideal point in the AEC method is about 19% less than in the NNC method. Additionally, the solution time and the general distance size of the solutions in the NNC method are 33% and 31% less than in the AEC method, respectively. The distribution of solutions in the NNC method is also 13% higher than in the AEC method.

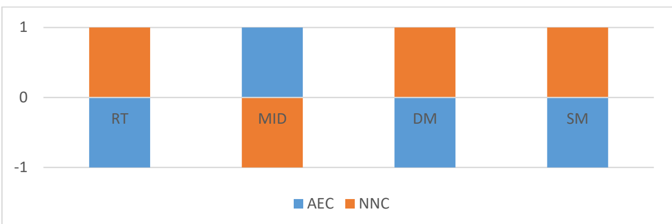

Figure 9: Comparison of attributes in AEC and NNC methods.

6 Conclusion

This problem involves conflicting objective functions, namely sustainability and reliability, alongside profitability and social responsibility. To address this conflict, a mixed integer linear programming model is formulated with sustainability dimensions as constraints and reliability as the primary objective. However, this single-objective approach may not effectively balance the conflicting objectives, resulting in an unsustainable or unreliable supply chain. To overcome this limitation, two methods (AEC and NNC) are utilized in multi-objective problems, and a numerical example with four different weights of objective functions is coded and modeled using GAMS software. The results of the AEC and the NNC methods were compared using the four criteria of Run Time (RT), Mean Ideal Distance (MID), Diversification Metric (DM), and Standard Deviation Metric (SDM). The Shannon Entropy technique is used to obtain the criteria weights, and the VIKOR technique is employed to select the superior method. The results indicate that the NNC method is more efficient than the AEC method in solving the proposed model. The NNC method exhibits several advantages over the AEC method, including a systematic approach to reducing feasible space and effectively covering the objective space through the uniform distribution of Pareto solutions. These capabilities enable the NNC method to discover more preferred multi-objective solutions compared to the AEC method. Previous research has focused on developing sustainable and reliable strategies for biofuel and blood supply chains. However, with a slight adjustment to the assumptions, these models can be applied to industries that require greater consideration of sustainability and reliability approaches, such as energy and healthcare. While past studies have primarily focused on sustainability's economic and environmental dimensions, there is a need to balance all three dimensions (economic, environmental, and social) for optimal benefits. In addition to greenhouse gas emissions and job creation, other criteria such as energy consumption, use of renewable resources, waste disposal, community well-being, safety, job satisfaction, and personnel training must also be considered for a comprehensive assessment of sustainability. Despite the growing trend of integrating sustainability and reliability in SCND literature, this topic is still a developing field that requires more empirical studies to formulate precise and long-term guidelines for simultaneous application. Future researchers can draw a roadmap by adding or changing problem assumptions, providing more criteria for evaluating solution methods, and using other multi-objective solving techniques.

Here are some suggestions for this road map: The proposed model assumes no distinction between goods produced with raw materials and those produced with recycled raw materials and thus accounts for differences in production costs, prices, and demand for these two types of products. While this study considered fixed and certain model parameters, incorporating uncertainty conditions can enhance the model's realism. To validate the model's performance, a numerical example and random data with a uniform distribution are provided, and the model's flexibility is examined through a real case study. Four criteria are used to evaluate the performance of problem-solving methods, and additional appropriate performance criteria are employed to compare and demonstrate the effectiveness of the proposed methods. The Shannon entropy method is utilized to weigh the evaluation criteria, and the weighting result is combined with several MCDM methods such as Best Worst Method (BWM) for a more comprehensive assessment of criterion weights.

Declarations

Availability of supporting data

All data generated or analyzed during this study are included in this published paper.

Funding

No funds, grants, or other support were received for conducting this study.

Competing interests

The authors have no competing interests to declare that are relevant to the content of this paper.

Authors' contributions

The main manuscript text is written collectively by the authors.

References

[1] Abir, A.S., Bhuiyan, I. A., Arani, M., Billal, M.M. (2020). "Multi-objective optimization for sustainable closed-loop supply chain network under demand uncertainty: A genetic algorithm", In 2020 International Conference on Data Analytics for Business and Industry: Way Towards a Sustainable Economy (ICDABI) (pp. 1-5). IEEE.

[2] Ahi, P., Searcy, C. (2015). "An analysis of metrics used to measure performance in green and sustainable supply chains", Journal of Cleaner Production, 86, 360-377.

[3] Ahmadigorji, M., Amjady, N., Dehghan, S. (2017). "A robust model for multiyear distribution network reinforcement planning based on information-gap decision theory", IEEE Transactions on Power Systems, 33(2), 1339-1351.

[4] Akbari-Kasgari, M., Khademi-Zare, H., Fakhrzad, M.B., Hajiaghaei-Keshteli, M., Honarvar, M. (2022). "Designing a resilient and sustainable closed-loop supply chain network in copper industry", Clean Technologies and Environmental Policy, 1-28.

[5] Amirian, S., Amiri, M., Taghavifard, M.T. (2022a). "The Emergence of a Sustainable and Reliable Supply Chain Paradigm in Supply Chain Network Design", Complexity, 2022.

[6] Amirian, S., Amiri, M., Taghavifard, M.T. (2022b). "Sustainable and reliable closed-loop supply chain network design: Normalized Normal Constraint (NNC) method application", Journal of Industrial and Systems Engineering, 14(3), 33-68.

[7] Basu, D., Lee, M. (2022). "A combined sustainability-reliability approach in geotechnical engineering", In Risk, Reliability and Sustainable Remediation in the Field of Civil and Environmental Engineering (pp. 379-413). Elsevier.

[8] Bektaş, T., Laporte, G. (2011). "The pollution-routing problem", Transportation Research Part B: Methodological, 45(8), 1232-1250.

[9] Boronoos, M., Mousazadeh, M., Torabi, S.A. (2021). "A robust mixed flexible-possibilistic programming approach for multi-objective closed-loop green supply chain network design", Environment, Development and Sustainability, 23(3), 3368-3395.

[10] Chambari, A., Rahmati, S.H.A., Najafi, A.A. (2012). "A bi-objective model to optimize reliability and cost of system with a choice of redundancy strategies", Computers & Industrial Engineering, 63(1), 109-119.

[11] Dullaert, W., Zamparini, L. (2013). "The impact of lead time reliability in freight transport: A logistics assessment of transport economics findings", Transportation Research Part E: Logistics and Transportation Review, 49(1), 190-200.

[12] Eslamipoor, R., Nobari, A. (2023). “A reliable and sustainable design of supply chain in healthcare under uncertainty regarding environmental impacts”, Journal of Applied Research on Industrial Engineering, 10(2), 256-272.

[13] Fakhrzad, M.B., Goodarzian, F. (2019). “A fuzzy multi-objective programming approach to develop a green closed-loop supply chain network design problem under uncertainty: modifications of imperialist competitive algorithm”, RAIRO-Operations Research, 53(3), 963-990.

[14] Fattahi, M., Govindan, K. (2018). “A multi-stage stochastic program for the sustainable design of biofuel supply chain networks under biomass supply uncertainty and disruption risk: A real-life case study”, Transportation Research Part E: Logistics and Transportation Review, 118, 534-567

[15] Fazli-Khalaf, M., Mirzazadeh, A., Pishvaee, M.S. (2017). “A robust fuzzy stochastic programming model for the design of a reliable green closed-loop supply chain network”, Human and Ecological Risk Assessment: an International Journal, 23(8), 2119-2149.

[16] Fazli-Khalaf, M., Naderi, B., Mohammadi, M., Pishvaee, M.S. (2020). “Design of a sustainable and reliable hydrogen supply chain network under mixed uncertainties: A case study”, International Journal of Hydrogen Energy, 45(59), 34503-34531.

[17] Fazli-Khalaf, M., Naderi, B., Mohammadi, M., Pishvaee, M.S. (2021). “The design of a resilient and sustainable maximal covering closed-loop supply chain network under hybrid uncertainties: A case study in tire industry”, Environment, Development and Sustainability, 23(7), 9949-9973.

[18] Foong, S.Z., Ng, D.K. (2022). “A systematic approach for synthesis and optimisation of sustainable oil palm value chain (OPVC)”, South African Journal of Chemical Engineering, 41, 65-78.

[19] Ghayebloo, S., Tarokh, M.J., Venkatadri, U., Diallo, C. (2015). “Developing a bi-objective model of the closed-loop supply chain network with green supplier selection and disassembly of products: The impact of parts reliability and product greenness on the recovery network”, Journal of Manufacturing Systems, 36, 76-86.

[20] Ghobakhloo, M., Iranmanesh, M., Mubarak, M.F., Mubarik, M., Rejeb, A., Nilashi, M. (2022). “Identifying industry 5.0 contributions to sustainable development: A strategy roadmap for delivering sustainability values”, Sustainable Production and Consumption, 33, 716-737.

[21] Gong, D.C., Chen, P.S., Lu, T.Y. (2017). “Multi-objective optimization of green supply chain network designs for transportation mode selection”, Scientia Iranica, 24(6), 3355-3370.

[22] Govindan, K., Gholizadeh, H. (2021). “Robust network design for sustainable-resilient reverse logistics network using big data: A case study of end-of-life vehicles”, Transportation Research Part E: Logistics and Transportation Review, 149, 102279.

[23] Govindan, K., Fattahi, M., Keyvanshokooh, E. (2017). “Supply chain network design under uncertainty: A comprehensive review and future research directions”, European Journal of Operational Research, 263(1), 108-141.

[24] Hamidieh, A., Naderi, B., Mohammadi, M., Fazli-Khalaf, M. (2017). “A robust possibilistic programming model for a responsive closed loop supply chain network design”, Cogent Mathematics, 4(1), 1329886.

[25] Hosseini-Motlagh, S.M., Samani, M.R.G., Shahbazbegian, V. (2020). “Innovative strategy to design a mixed resilient-sustainable electricity supply chain network under uncertainty”, Applied Energy, 280, 115921.

[26] Ivanov, D., Das, A. (2020). “Coronavirus (COVID-19/SARS-CoV-2) and supply chain resilience: A research note”, International Journal of Integrated Supply Management, 13(1), 90-102.

[27] Jabbarzadeh, A., Fahimnia, B., Sabouhi, F. (2018). "Resilient and sustainable supply chain design: Sustainability analysis under disruption risks", International Journal of Production Research, 56(17), 5945-5968.

[28] Kabadurmus, O., Erdogan, M.S. (2020). "Sustainable, multimodal and reliable supply chain design", Annals of Operations Research, 292(1), 47-70.

[29] Kaur, H., Singh, S.P. (2019). "Sustainable procurement and logistics for disaster resilient supply chain", Annals of Operations Research, 283(1), 309-354.

[30] Khosravi, K., Pourghasemi, H.R., Chapi, K., Bahri, M. (2016). "Flash flood susceptibility analysis and its mapping using different bivariate models in Iran: A comparison between Shannon's entropy, statistical index, and weighting factor models", Environmental Monitoring and Assessment, 188(12), 1-21.

[31] Li, Q., Loy-Benitez, J., Nam, K., Hwangbo, S., Rashidi, J., Yoo, C. (2019). "Sustainable and reliable design of reverse osmosis desalination with hybrid renewable energy systems through supply chain forecasting using recurrent neural networks", Energy, 178, 277-292.

[32] Liu, J., Feng, Y., Zhu, Q., Sarkis, J. (2018). "Green supply chain management and the circular economy: Reviewing theory for advancement of both fields", International Journal of Physical Distribution & Logistics Management, 48(8), 794 - 817.

[33] Marchi, B., Zanoni, S., Zavanella, L.E., Jaber, M.Y. (2019). "Supply chain models with greenhouse gases emissions, energy usage, imperfect process under different coordination decisions", International Journal of Production Economics, 211, 145-153.

[34] Mavrotas, G. (2009). "Effective implementation of the ε-constraint method in multi-objective mathematical programming problems", Applied Mathematics and Computation, 213(2), 455-465.

[35] Mavrotas, G., Florios, K. (2013). "An improved version of the augmented ε-constraint method (AUGMECON2) for finding the exact Pareto set in multi-objective integer programming problems", Applied Mathematics and Computation, 219(18), 9652-9669.

[36] Messac, A., Mattson, C.A. (2004). "Normal constraint method with guarantee of even representation of complete Pareto frontier", AIAA Journal, 42(10), 2101-2111.

[37] Mirzapour Al-e-hashem, S.M.J., Rekik, Y. (2014). "Multi-product multi-period inventory routing problem with a transshipment option: A green approach", International Journal of Production Economics, 157, 80-88.

[38] Mousavi Ahranjani, P., Ghaderi, S.F., Azadeh, A., Babazadeh, R. (2020). "Robust design of a sustainable and resilient bioethanol supply chain under operational and disruption risks", Clean Technologies and Environmental Policy, 22(1), 119-151.

[39] Nosrati, M., Khamseh, A. (2020). "Reliability optimization in a four-echelon green closed-loop supply chain network considering stochastic demand and carbon price", Uncertain Supply Chain Management, 8(3), 457-472.

[40] Pereira, J.L.J., Oliver, G.A., Francisco, M.B., Cunha, S.S., Gomes, G.F. (2021). "A review of multi-objective optimization: methods and algorithms in mechanical engineering problems", Archives of Computational Methods in Engineering, 1-24.

[41] Rahmani, S., Amjady, N. (2018). "Improved normalized normal constraint method to solve multi-objective optimal power flow problem", IET Generation, Transmission & Distribution, 12(4), 859-872.

[42] Rahmani, D., Mahoodian, V. (2017). "Strategic and operational supply chain network design to reduce carbon emission considering reliability and robustness", Journal of Cleaner Production, 149, 607-620.

[43] Rohaninejad, M., Sahraeian, R., Tavakkoli-Moghaddam, R. (2018). “Multi-echelon supply chain design considering unreliable facilities with facility hardening possibility”, Applied Mathematical Modelling, 62, 321-337.

[44] Salehi, M., Jabarpour, E. (2020). “Modeling and solving a multi-objective location-routing problem considering the evacuation of casualties and homeless people and fuzzy paths in relief logistics”, Control and Optimization in Applied Mathematics, 5(1), 41-65.

[45] Sundarakani, B., De Souza, R., Goh, M., Wagner, S.M., Manikandan, S. (2010). “Modeling carbon footprints across the supply chain”, International Journal of Production Economics, 128(1), 43-50.

[46] Tao, J., Shao, L., Guan, Z., Ho, W., Talluri, S. (2020). “Incorporating risk aversion and fairness considerations into procurement and distribution decisions in a supply chain”, International Journal of Production Research, 58(7), 1950-1967.

[47] Tirkolaee, E.B., Mardani, A., Dashtian, Z., Soltani, M., Weber, G.W. (2020). “A novel hybrid method using fuzzy decision making and multi-objective programming for sustainable-reliable supplier selection in two-echelon supply chain design”, Journal of Cleaner Production, 250, 119517.

[48] Torjai, L., Nagy, J., Bai, A. (2015). “Decision hierarchy, competitive priorities and indicators in large-scale ‘herbaceous biomass to energy supply chains”, Biomass and Bioenergy, 80, 321-329.

[49] Wang, F., Lai, X., Shi, N. (2011). “A multi-objective optimization for green supply chain network design”, Decision Support Systems, 51(2), 262-269.

[50] Wang, B., Zhang, H., Yuan, M., Guo, Z., Liang, Y. (2020). “Sustainable refined products supply chain: a reliability assessment for demand side management in primary distribution processes”, Energy Science & Engineering, 8(4), 1029-1049.

[51] Yılmaz, Ö.F., Özçelik, G., Yeni, F.B. (2021). “Ensuring sustainability in the reverse supply chain in case of the ripple effect: A two-stage stochastic optimization model”, Journal of Cleaner Production, 282, 124548.

[52] Zahiri, B., Zhuang, J., Mohammadi, M. (2017). “Toward an integrated sustainable-resilient supply chain: A pharmaceutical case study”, Transportation Research Part E: Logistics and Transportation Review, 103, 109-142.

[53] Zitzler, E., Thiele, L. (1998). “Multi-objective optimization using evolutionary algorithms—a comparative case study”, In International Conference on Parallel Problem Solving from Nature (pp. 292-301). Springer, Berlin, Heidelberg.